

MODELLING THE HYDRAULIC LIFT PHENOMENON DURING CASING WHILE DRILLING

SAIFUL ISLAM

MASTER OF ENGINEERING IN PETROLEUM ENGINEERING



DEPARTMENT OF PETROLEUM AND MINERAL RESOURCES ENGINEERING

BANGLADESH UNIVERSITY OF ENGINEERING AND TECHNOLOGY

DHAKA, BANGLADESH

DECEMBER, 2015

MODELLING THE HYDRAULIC LIFT PHENOMENON DURING
CASING WHILE DRILLING

A PROJECT BY

SAIFUL ISLAM


SUBMITTED TO THE
DEPARTMENT OF PETROLEUM AND MINERAL RESOURCES ENGINEERING
BANGLADESH UNIVERSITY OF ENGINEERING AND TECHNOLOGY
IN PARTIAL FULFILLMENT OF THE REQUIREMENTS FOR THE DEGREE OF
MASTER OF ENGINEERING IN PETROLEUM ENGINEERING

DECEMBER, 2015


RECOMMENDATION OF THE BOARD OF EXAMINERS

The project entitled as “**MODELLING THE HYDRAULIC LIFT PHENOMENON DURING CASING WHILE DRILLING**” submitted by Saiful Islam, Roll No: 0413132023 F, Session April/2013 has been accepted as satisfactory in partial fulfillment of the requirements for the degree of **Master of Engineering in Petroleum Engineering** on December 23, 2015.

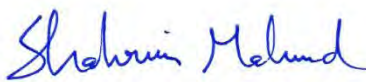
Chairman (Supervisor) :


:
Mohammad Mojammel Huque
Assistant Professor
Department of PMRE, BUET, Dhaka.

Member :


:
Dr. Mohammad Tamim
Professor
Department of PMRE, BUET, Dhaka.

Member :


:
Shahriar Mahmud
Assistant Rig Manager
KCA Deutag, Myanmar.

Date: December 23, 2015

Declaration

It is hereby declared that this project or any part of it has not been submitted elsewhere for the award of any degree or diploma.

Saiful Islam

Saiful Islam

Abstract

Casing while Drilling (CwD) is a process in which a well is drilled and cased simultaneously. This innovative technology has been successfully practiced for the past decade. However, narrow annuli often causes problems like packing or caving in the wellbore that may restrict the fluid flow and hole cleaning capacity. Hydraulic lift could be one of the beneficial factors that can be used to increase the efficiency of drilling as it can be used to monitor the wellbore condition. The purpose of this project work is to develop a theoretical model to calculate the overall hydraulic lift during CwD to evaluate the wellbore irregularities.

As CwD process utilizes large diameter casing to drill, several forces act upwards on the casing. Usually Small annulus brings about higher frictional pressure drop compare to the conventional operation that causes high upward drag force on casing wall. Another force acts upwards at the bottom face of the casing while fluid exits through the nozzles. In this study fluid hydraulic principles have been used to generate the overall hydraulic lift model. This theoretical model has then been compared with field measurement from hookload. Deviation of the field measured value from the predicted hydraulic lift is an indicator of wellbore conditions.

In this study trend of hydraulic lift predicted using theoretical model is compared with the field measured value of an well. Observation of this comparison is then analyzed with the field report to validate the model. Hydraulic lifts for three different depth interval and flow rates are measured. Findings of the comparisons are correlated with the summary of the field report for each section. Most significant finding is higher field measured hydraulic lift means higher friction due to packing or caving from the well bore that resembles the field observation also for a certain interval. The novelty of using hydraulic lift in CwD will enable the monitoring of wellbore condition to improve hole cleaning efficiency during operation.

Acknowledgement

This project work became possible with suggestions and encouragements of several precious people during my two years of master's study. Without their support, this study would not have been possible.

First of all I would like to thank my supervisor Mohammad Mojammel Huque, Assistant Professor, Department of Petroleum & Mineral Resources Engineering, Bangladesh University of Engineering and Technology for his supervision, guidance, encouragement, reviewing throughout this work.

I also would like to express my deepest and sincerest thank to Mr. Shahriar Mahmud, Assistant Rig Manager, KCA Deutag, Myanmar for many reasons. First of all for selecting such an interesting topic and then constantly supervising me with proper directions and providing useful information.

I am grateful to Dr. Mohammad Tamim, Professor and Head, Department of Petroleum & Mineral Resources Engineering, Bangladesh University of Engineering and Technology for his valuable advice, guidance and inspiration during his lectures that help me a lot in completing this work.

Then I have to mention Mr. Moji Karimi, Product Launch Manager, Weatherford, USA who has supported me in getting necessary data and information.

LIST OF CONTENTS

CHAPTER 1: INTRODUCTION	1
1.1 Purpose of the work.....	1
1.2 Background of the study.....	1
CHAPTER: 2 LITERATURE REVIEW	3
2.1 Casing while Drilling Technology.....	3
2.2 Casing while Drilling features.....	4
2.3 Advantages of Casing while Drilling Technology.....	7
2.3.1 Reduce Drilling Times.....	8
2.3.2 Elimination of swab and surge pressure effects.....	8
2.3.3 Rig adaptations and HSE.....	9
2.3.4 Effective borehole cleaning.....	9
2.3.5 Wellbore in gauge.....	10
2.3.6 Improvements on production.....	12
2.3.7 Lost circulation reduction.....	12
2.3.8 Reduce cost of the well.....	13
2.4 Limitations of Casing while Drilling Technology.....	14
2.5 Review of hydraulics.....	15
2.5.1 Drilling Fluid Rheology.....	15
2.5.2 Fluid Flow and Frictional Pressure Loss Analysis for a CwD annulus.....	18
2.5.3 Annular Frictional Pressure Loss using Narrow Slot Approximation method....	19
CHAPTER 3: METHODOLOGY	22
3.1 Hydraulic lift phenomenon.....	22
3.2 Model Description.....	23
3.2.1 Model derivation for vertical well with uniform casing and hole.....	25
3.2.2 Model derivation with liner.....	27
3.2.3 Model derivation for inclined well	29
3.2.4 Field Measuring Procedure of Hydraulic Lift.....	31
CHAPTER 4: CASE STUDIES	32
4.1 Background of the field.....	35
4.2 Factors affecting hydraulic lift.....	35
4.2.1 Effect of mud flow rate.....	37

4.2.2 Effect of borehole size.....	38
4.2.3 Effect of cuttings concentration.....	38
4.2.4 Criteria to evaluate predicted and measured.....	39
4.3 Result analysis of the predicted and field measured value.....	43
4.3.1 Study of HL using the model at depth 8715-8750 ft- Section I.....	44
4.3.2 Study of HL using the model at depth 8770-9180 ft- Section II.....	46
4.3.3 Study of HL using the model at depth 9190-9204 ft- Section III.....	51
CHAPTER 5: CONCLUSION.....	56
REFERENCES.....	58
APPENDICES.....	60

LIST OF FIGURES

Figure 2.1: a) Non Retrievable CwD assembly and b) Conventional drilling assembly (Karimi et al 2012)	5
Figure 2.2: Casing Drive System mounted to top drive (Warren et al.,2004).....	6
Figure 2.3: Retrievable CwD Bottom Hole Assembly set for directional drilling (Warren and Lesso, 2005).....	7
Figure 2.4: Drilling days between conventional drilling and casing drilling (Lopez and Bonilla, 2010).....	9
Figure 2.5: Differences between conventional drilling and casing drilling annulus size (Moellendick and Karimi, 2011).....	10
Figure2.6: Borehole quality improvement by CwD (right) as compared to conventional drilling(left).....	11
Figure2.7: Contact angle of CwD (right) is smaller than contact angle of drill pipe (left) $\alpha_1 > \alpha_2$, α = contact angle of the pipe with the wellbore(Karimi et al., 2011)...	12
Figure2.8: Contact area of CwD (right) is smaller than contact area of drill pipe (left) $A_1 < A_2$, A = contact area of the pipe with the wellbore(Karimi et al., 2011)...	12
Figure2.9: Penetration depth onto filter cake, penetration of CwD is less than penetration of drill pipe $d_1 > d_2$; d = penetration depth into the filter cake (Karimi et al.,2011).....	12
Figure 2.10: Wells drilled with CwD outperformed conventional wells in gas production (Tessari et al.,2006).....	13
Figure 2.11: Casing drilling eliminates lost circulation (Karimi et al., 2011).....	14
Figure 2.12: Comparison Cost/ft between casing drilling wells and loss circulation wells (Lopez and Bonilla, 2010).....	15
Figure 2.13: Shear stress-Shear rate curve for different fluid types (Taken from Amoco Production Company – Drilling Fluids Manual).....	18
Figure 2.14: Representing the annulus as a slot: (a) annular and (b)equivalent slot expressing.....	21
Figure 3.1: Major contributing forces on Hydraulic Lift.....	23
Figure 3.2: Mud circulation system.....	25
Figure 3.3: Contributing forces on hydraulic lift (Vertical Well).....	26
Figure 3.4: Schematic of a Typical Liner drilling wellbore.....	29

Figure 3.5: Contributing forces on hydraulic lift in inclined well.....	20
Figure 4.1: Figure 4.1: Wellbore geometry of the well to be analyzed.....	34
Figure 4.2: Effect of flow rate on HL.....	37
Figure 4.3 Effect of hole size on HL	38
Figure 4.4: Effect of cuttings concentration on HL.....	39
Figure 4.5: Well bore geometry used in HL measurement.....	41
Figure 4.6: HL vs Measured depth at flow rate 293 gpm.....	43
Figure 4.7: Comparison between measured HL and predicted HL for depth 810 -8735 ft with flow rate 293 gpm	46
Figure 4.8: HL vs measured depth at flow rate 318 gpm.....	48
Figure 4.9: Comparison between measured HL and predicted HL for depth 810 -8735 ft with flow rate 318 gpm.....	51
Figure 4.10: HL vs Measured depth at flow rate 342 gpm.....	53
Figure 4.11: Comparison between measured HL and predicted HL for depth 810ft – 8735 ft with flow rate 293 gpm.....	56

LIST OF TABLES

Table 2.1: Summary of formulas for annulus frictional pressure drop.....	22
Table 4.1: Well parameters (Source: Weatherford International).....	35
Table 4.2: Mud properties (Source: Weatherford International).....	35
Table 4.3: Summary of the casing drilling operation (Source:Weatherford International)	34
Table 4.4: Different flow rates used to show the effect.....	37
Table 4.5: Well bore parameters used to show the effect of hole size.....	38
Table 4.6: Properties used to show the effect of cuttings.....	39
Table 4.7: Flow rates at different interval depth.....	40
Table 4.8: Parameter used in the model for flow rate 293 gpm.....	42
Table 4.9: HL calculation for 8710- 8735 ft.....	44
Table 4.10: Field measurement of HL at depth 8715-8713ft and flow rate 293gpm.....	45
Table 4.11: Parameter used in the model for flow rate 318 gpm.....	48
Table 4.12: HL calculation for 8770-9190 ft.....	49
Table4.13: Field measurement of HL at depth 8770-9180 ft and flow rate 318gpm.....	50
Table 4.14: Parameter used in the model for flow rate 342 gpm.....	53
Table 4.15: HL calculation for 9190 ft -9204 ft.....	54
Table 4.16: Field measurement of HL at depth 8715ft and flow rate 342gpm.....	55

Nomenclatures

BHA = Bore hole assembly

CwD = Casing while drilling

Cc = Cuttings concentration

D = Measured depth, ft

DwC= Drilling while Casing

d_c = Diameter of the casing, inch

d_h = Diameter of the hole, inch

$\frac{dp}{dl}$ = Frictional pressure drop, psi/ft

ECD= Equivalent circulating density, lbm/gal

F_1 =Frictional drag force on casing wall, kip

F_2 =End force at bottom of the casing face, kip

F_T = Cuttings transport ratio

f_f = Friction factor

He = Hedstorm number

HL = Hydraulic lift, kip

Gpm= Gallon per minute

K = Consistency index, dimensionless

N = Flow behavior index, dimensionless

N_{Re} = Reynolds number, dimensionless

NPT= Non Producing Time

PV = Plastic viscosity

Q = Flow rate, gpm

ROP = Rate of penetration, ft/hr

r_2 = Hole radius in narrow slot approximation, inch

r_1 = Casing radius in narrow slot approximation, inch

τ = Shear stress, psi

μ = Viscosity, cp

ρ_m = Mud density, lbm/gal

ρ_m = Effective mud density, lbm/gal

ρ_f = Mixture density, lbm/gal

θ = Inclination angle

YP = Yield point

v = velocity, ft/sec

V_{sl} = Particles slip velocity, ft/sec

v_a = Annular velocity, ft/sec

WOB = Weight on bit, lbf

CHAPATER 1: INTRODUCTION

1.1 Purpose of the work

Globally rising demand for oil and natural gas, and an increasing rate of depletion in producing reserves, lead the oil and gas industry continuously to find new techniques to improve drilling technology. Casing while Drilling (CwD) technology stands as a response to practical needs of the industry. The innovative CwD method eliminates the need for wiper trips prior to casing/cementing operations, because the casing string is already run in the hole as the well is being drilled. Therefore, it helps to reduce nonproductive time in the drilling operations. However, as CwD process utilizes large diameter casing to drill narrow annulus often hinders the mud flow and lead to reduce hole cleaning efficiency. These challenges demand innovative techniques in order to mitigate those problems.

Objectives

The aim of this project work is to derive a theoretical model of hydraulic lift phenomenon during operation. This model can be used as a basic tool to understand the borehole conditions in CwD. The objectives of the study is to -

- (i) Generate a theoretical model of total upward hydraulic lifting force during CwD.
- (ii) Measurement of the overall hydraulic lift using proposed theoretical model and observe the trend with respect to measured depth.
- (iii) Graphical comparisons of the trend of total upward lifting forces between fields measured value and calculated value.
- (iv) Examine the hole condition and cleaning efficiency during CwD in order to improve the wellbore conditions.

1.2 Background of the study

CwD is an innovative drilling method wherein the well is drilled and cased simultaneously. Historically, drilling design has been based on conventional drilling geometry; however, in time casing drilling has been becoming one of the industry's best practices. CwD introduces new benefits that modify conventional practices and offer a safer engineering design. Conoco-Philips was the first to imply the retrievable CwD technology in Lobo Trend in South Texas in 2012. Shell was the other company to apply the non-retrievable CwD technology successively in the same basin as a part of underbalanced drilling with casing operations. Apart from the hazard mitigation, one of the key factors that attract operators to drilling with casing is its capability to eliminate the casing running process in conventional drilling. The single operation removes nonproductive time and increase drilling efficiency. Reducing time for drilling operations also can bring significant cost savings. Plastering effect, another factor was observed in CwD operations completed in different formations that reduce the formation damage and lost circulation significantly compare to the conventional operation. As the technology has become widespread, various features also have arisen and hydraulic lift is one of these unique features.

To drill consistently it is always important to maintain better wellbore condition. Poor well bore often reduces the hole cleaning efficiency and causes the reduction of ROP. In order to mitigate these challenges hydraulic lift mode will be an useful tool to monitor the wellbore condition.

CHAPTER 2: LITERATURE REVIEW

In this chapter, aspects related to the CwD technology are introduced with the benefits and limitations explained. Furthermore, relevant theories of casing drilling fluid hydraulics are also described.

2.1 Casing while drilling technology

CwD technology is an emerging drilling technique that eliminates the need for the conventional drill string consisting of drill pipes, heavy weight drill pipes and drill collars in the drilling operations. Instead, this method utilizes a special bottom hole assembly connected to casing (Sanchez and Al-Harthy, 2011). Figure 2.1 shows the differences in the drill string geometry. Over the last decade, the CwD technology has worked satisfactorily in the contemporary drilling environments and has gained great interest, as it decreased non-productive time such as trips, casing operations, etc. of drilling operations. Along with the implementation of this technology, numerous facts about drilling with a larger sized diameter tubular have appeared. The benefits associated to the CwD technology that can be listed as bellow (Sanchez and Al-Harthy, 2011; Karimi et al., 2011; Rosenberg et al., 2010; Karimi et al., 2012).

- Improved well economics
- Borehole stability
- Wellbore integrity
- Reduction in number of casing/liner strings
- Personal safety and overall drilling efficiency

These benefits accelerated the research and development initiatives on the technology. Most of these benefits are supposedly related to the plastering effect of CwD.

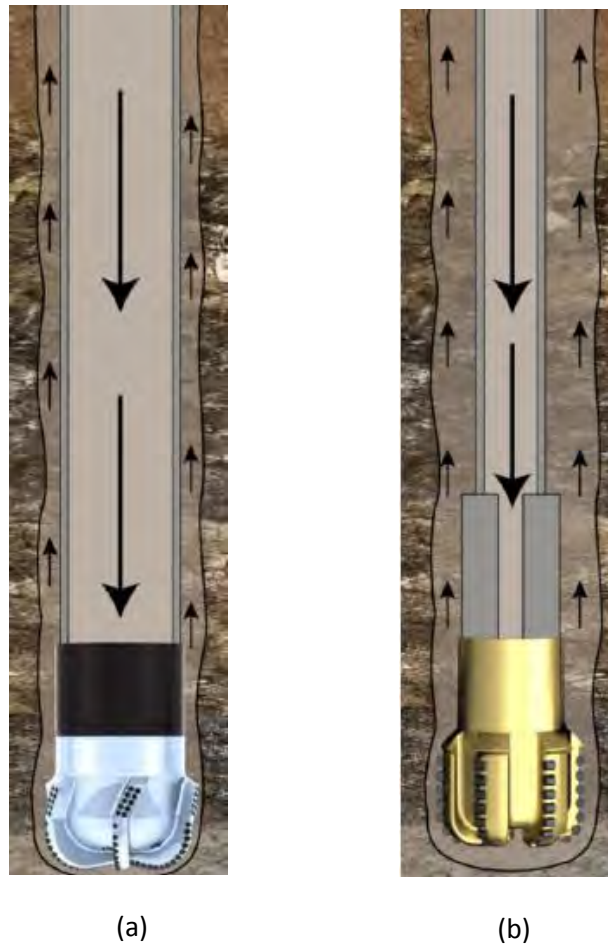


Figure 2.1 : a) Non Retrieveable CwD assembly and b) Conventional drilling assembly
(Karim et al 2012)

2.2 Casing while Drilling features

CwD essentially drills the hole by using a casing string as the drill string. Since actual drilling is conducted with the casing itself, the well is automatically cased and ready to cement once the target casing depth is reached. Usually regular casings in API standards are durable enough to satisfy operating conditions. Based on the weight on bit (WOB) requirements and torque-drag conditions, special accessories such as wear bands and torque rings can be installed in connections (Gupta, 2006).

CwD technology must be employed with several modifications in the rig set up. Most importantly, an automated drive system must be mounted to the top drive mechanism to safely connect individual casings to the string. This system is responsible for pipe

handling, connection, transfer of motion and transfer of fluid flow. The surface casing drive system mounted to top drive grabs the individual casing internally via a spear ball and externally via a slip mechanism, and makes connection and transfer of fluid through inside casing. Also it seals the casing and prevents leaks in drilling fluid transfer (Warren et al., 2004). Figure 2.2 shows a casing drive system. In addition to the casing drive mechanism, size and capacity of the rig can be reduced. Since trips will be eliminated, the hoisting system elements can be modified. Mud pump capacities can be decreased as well. Overall, these changes make the rig more practical by making it easier and faster to transport and to set up. The wellhead equipment and blowout preventer configuration must also be appropriate for large sized tubular (Gupta, 2006).



Figure 2.2: Casing Drive System mounted to top drive (Warren et al., 2004)

The CwD technology is commonly practiced with two methods; non-retrievable CwD and retrievable CwD. Operational procedure of the non-retrievable CwD system includes a drillable drilling bit attached to the casing string with float collar rigid

stabilizers installed on it. Once the target depth is reached, cutters and steel blades are pushed out of the drilling path and the aluminum portion of the bit stays in place. Cementing is conducted through this portion, and the new section starts by drilling through the remaining parts of PDC bit in place and rat hole with the new drill string (Kenga et al. 2009).

On the other hand, the retrievable CwD system utilizes a custom bottom hole assembly (BHA) set up assembled to casing string with drill lock assembly. The specific BHA includes a pilot PDC bit and underreamer. Optionally it can include a down hole motor, MWD tools and a configuration of stabilizers. The PDC bit drills the pilot hole and underreamer enlarges the wellbore to its final shape. The drill lock assembly transfers motion from casing string to BHA. The retrievable CwD offers the flexibility of changing drill bit. Based on the necessity, BHA can be pulled and run into the hole by wireline or drillpipes. Figure 2.3 shows a model BHA for the retrievable CwD system. The selection of the proper method is based on drillability of the interval of interest with single-run (can be estimated according to the previous bit records, drilling parameters and logs) or trajectory requirements of the wellbore (Kenga et al., 2009).

From an engineering standpoint, the application of this technology requires deep understanding of the technology and a systematic approach in drilling operations. It is required to divide the operation into three phases: pre-operation phase, drilling phase and post-operation phase. In the pre-operation phase, the limitations and risks induced by field properties must be well examined. Approximate drilling fluid parameters and wellbore geometry are designed in this phase. Also, correlation to the other wells helps to detect problematic sections. During the actual drilling phase, the operation must be tracked meticulously. Using fundamental drilling engineering concepts and effective practices, real-time parameters must be managed and key components must be updated. Surface pressure, drilling fluid returns, ROP, bit performance, and torque and drag are important parameters to control in this step. The post-operation phase must aim to perform efficiency review sessions and to enhance the applied technology with the new ideas and the contribution of various technologies based on evaluation of the operation. Successful results and development of this technology are not guaranteed if these conditions are ignored (Sanchez et al., 2011).

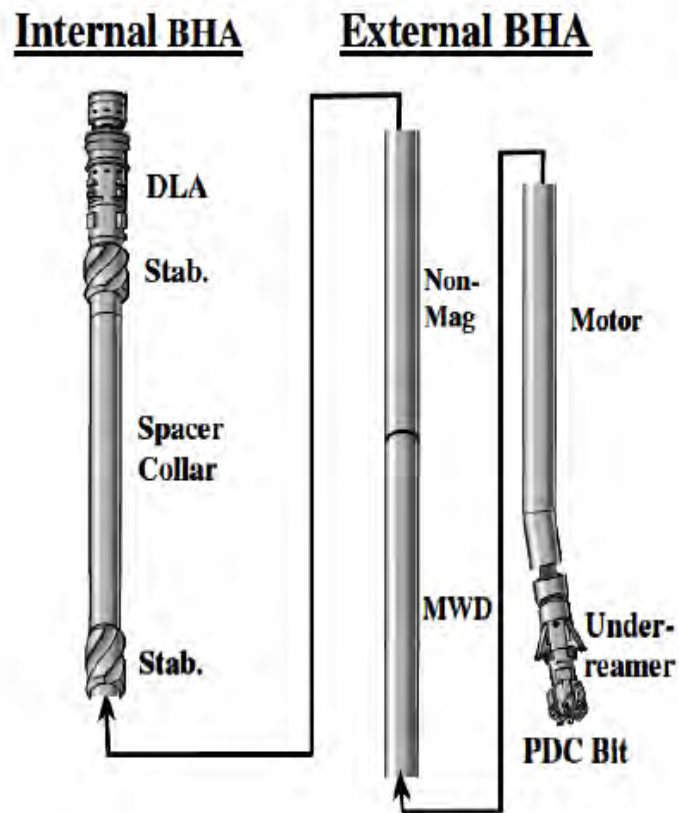


Figure 2.3: Retrievable CwD Bottom Hole Assembly set for directional drilling
(Warren and Lesso, 2005)

2.3 Advantages of casing while drilling technology

Casing drilling has several benefits in mitigating wellbore stability problems and lost circulation situations. Thus, it is often chosen rather than a conventional drilling process. Casing drilling eliminates unexpected events that often accompany conventional drilling and its tripping problems. The most important benefits of casing drilling are given below

- Reduce Drilling Times
- Elimination of swab and surge effects
- Rig adaptation and HSE
- Wellbores in gauge

- Effective borehole cleaning
- Improvements on production
- Lost circulation reduction

2.3.1 Reduce drilling times

Casing drilling reduces the total non-productive drilling times associated with tripping, running casing, and lost circulation problems. Figure 2.4 compares drilling days using casing drilling and conventional drilling in pressure depleted La Cira Infantas mature field, Columbia which indicates that casing drilling reduces drilling times by 20% compared to conventional drilling (Lopez et al 2010).

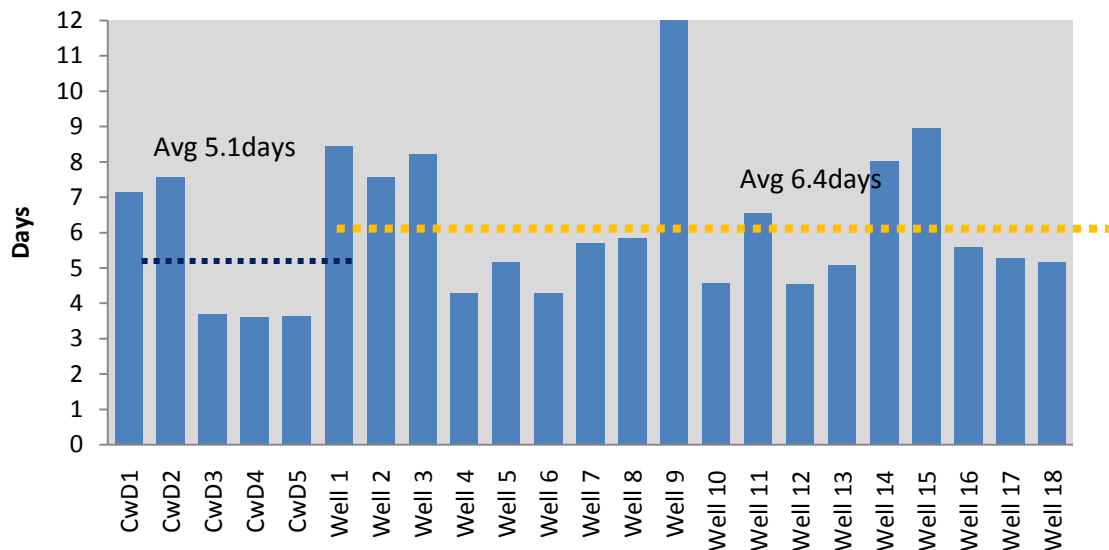


Figure 2.4: Drilling days between conventional drilling and casing drilling (Lopez and Bonilla, 2010)

2.3.2 Elimination of swab and surge pressure effects

There is no need to trip the drill string in casing drilling; As the casing is at the bottom it is ready to be cemented. This eliminates swab and surge pressures also that accompany tripping operations.

2.3.3 Rig adaptations and HSE

A custom designed rig for the CwD application is more practical and efficient than the conventional rig set up. The rig adaptation guidelines for CwD eliminate the need for greater horsepower in rig units. Hoisting systems and mud pumps can be redesigned considering the specific conditions of CwD. Also, these types of rigs require capability to lift only a single joint, reducing the mast height. After all these modifications, the rig turns into cutting edge technology machines, which are more practical, and easier to move and rig up. In addition to that, the time spent on mobilization, transfer and rig up and logistic services are improved. Besides ease in operability, the well site safety is improved with automated systems and incidents while handling pipes are lessened (Gupta, 2006).

2.3.4 Effective borehole cleaning

Casing drilling generates more effective borehole cleaning during drilling. The cuttings are circulated out with the high annular velocity that increases the borehole cleaning efficiency because of smaller clearance between the casing wall and the borehole wall. Consequently, stuck pipe problem do not occur. The small clearance between the casing and borehole is shown in Figure 2.5.

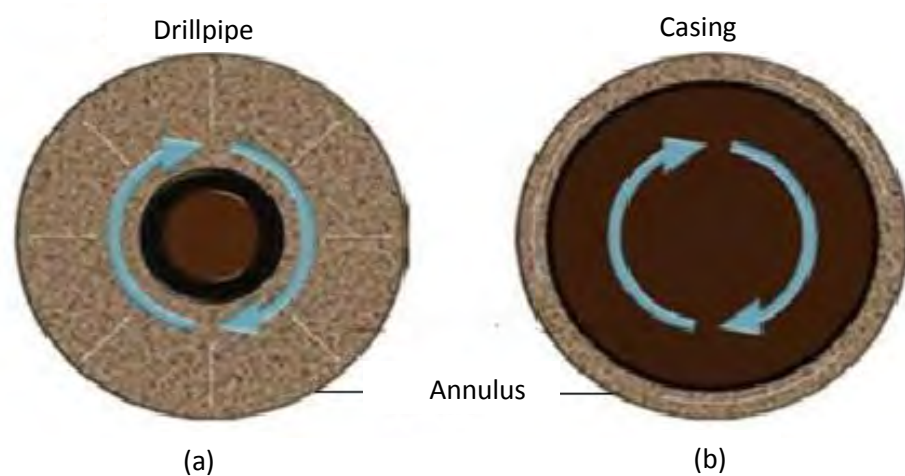


Figure 2.5: Differences between conventional drilling (a) and casing drilling annulus size (b) (Karimi et al, 2011)

2.3.4 Wellbores in gauge

In drilling operations, the gauged holes are preferred because they enable effective cementing operations and improved wellbore cleaning with superior hydraulics. The CwD pipe geometry tends to create a gauged well by means of the smooth rotational motion of casing. Figure 2.6 represents an example of the difference between a conventionally drilled well and a casing drilled well. The physical explanation beyond CwD-offered better wellbores consists of casing contact angle and area of the casing in contact with wellbore and penetration depth into filter cake. During the CwD process the casing string hits the borehole with a smaller contact angle and greater contact area. This action combines the side force and momentum of the pipe with grinding effect to generate a more circular wellbore; and potentially help to fill in washouts and breakouts. From the penetration depth into filter cake standpoint, when compared to drilling with drill pipe, casing will have the same force due to rotation of the pipe; yet, the area on which it is applied is greater. Thus, pressure applied on the wellbore by physical contact of casing will be moderate and that will rub filter cake instead of damaging through it. Figure 2.7, 2.8 and 2.9 illustrates the comparisons of wellbore geometry between CwD and conventional drilling based on contact area, contact angle and penetration depth into filter cake (Karimi et al. 2011).



Figure 2.6: Borehole quality improvement by compared to conventional drilling (a)

CwD (b)

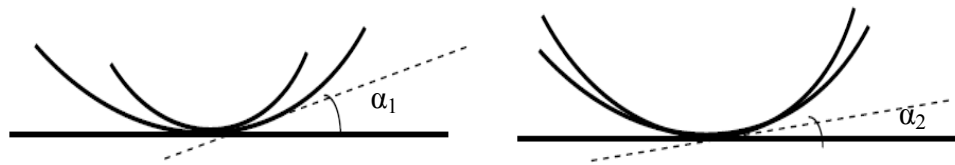


Figure 2.7: Contact angle of CwD (right) is smaller than contact angle of drill pipe (left) $\alpha_1 > \alpha_2$, α = contact angle of the pipe with the wellbore (Karimi et al., 2011)



Figure 2.8: Contact area of CwD (right) is smaller than contact area of drill pipe (left) $A_1 < A_2$, A = contact area of the pipe with the wellbore(Karimi et al., 2011)



Figure 2.9: Penetration depth onto filter cake, penetration of CwD (right) is less than penetration of drill pipe (left) $d_1 > d_2$; d = penetration depth into the filter cake (Karimi et al., 2011)

2.3.6 Improvements on production

One of the striking benefits of this technology is observed in reduced formation damage and better production performance. Lost circulation damages production zones while drilling. Casing drilling prevents lost circulation and fluid invasion due to the plastering effect. This results in a better production rate than conventional drilling. To understand the effect following scenario can be considered. Figure 2.10 compares seventeen conventional well production drilled in 2000 with twenty eight casing drilled wells in 2004 in south Texas (Tessari et al 2006). Over the period of time production rate was higher for CwD

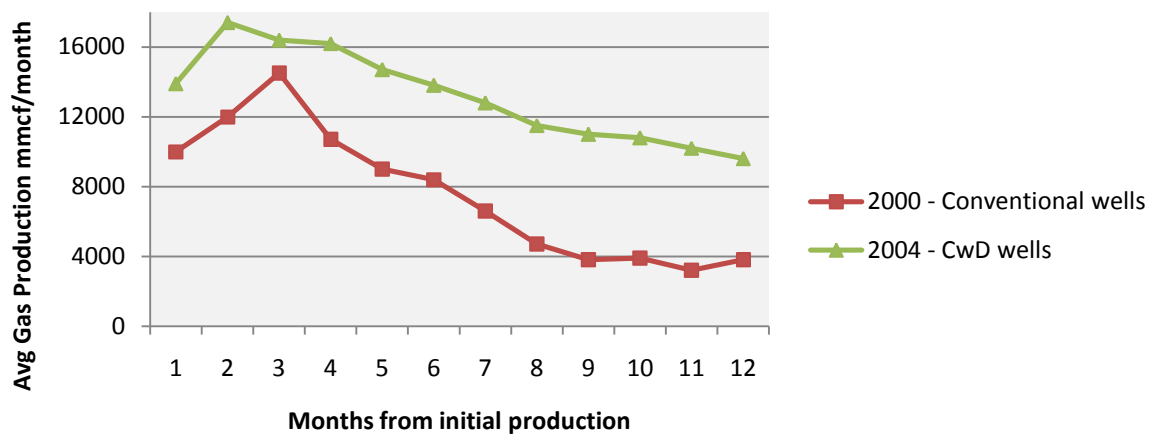


Figure 2.10: Wells drilled with CwD outperformed conventional wells in gas production (Tessari et al.,2006)

2.3.7 Lost circulation reduction

Casing drilling with its plastering effect reduces lost circulation and improves wellbore stability. It was observed that lost circulation was eliminated by casing drilling in the Lobo Field in South Texas in 2002. Figure 2.11 shows the wells that had lost circulation which was eliminated by casing drilling. First three wells were drilled conventionally in a particular zone which encountered extensive lost circulation. While casing drilling was run within this zone found no difficulties of lost circulation. The casing drilling required 10 days to drill 7” casing point and cement

the casing as compared to the first offset which required 19 days to reach an equivalent point. (Karimi et al., 2011)

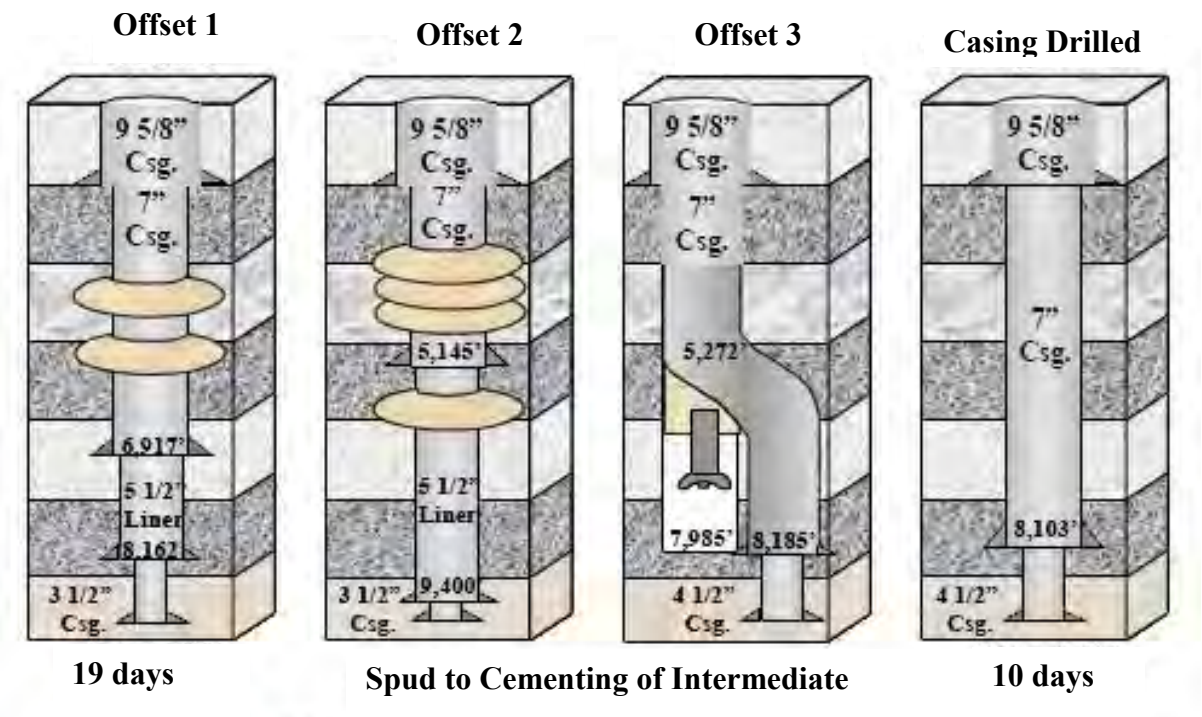


Figure 2.11: Casing drilling eliminates lost circulation (Karimi et al., 2011)

2.3.8 Reduce cost of the well

Casing drilling is generally applied to wells that have lost circulation and wellbore stability problems. Both in onshore and offshore drilling, daily rig costs are high and drilling problems are expensive. Since casing drilling eliminates or minimizes lost circulation and wellbore problems, the non-productive time is less. Figure 2.12 presents a comparison between casing drilling and loss circulation wells in cost/ft in depleted La Cira Infantas mature field in Colombia .and found that the casing drilling reduced the cost of drilling by about 12% compared to conventional drilling. (Lopez and Bonilla 2010)

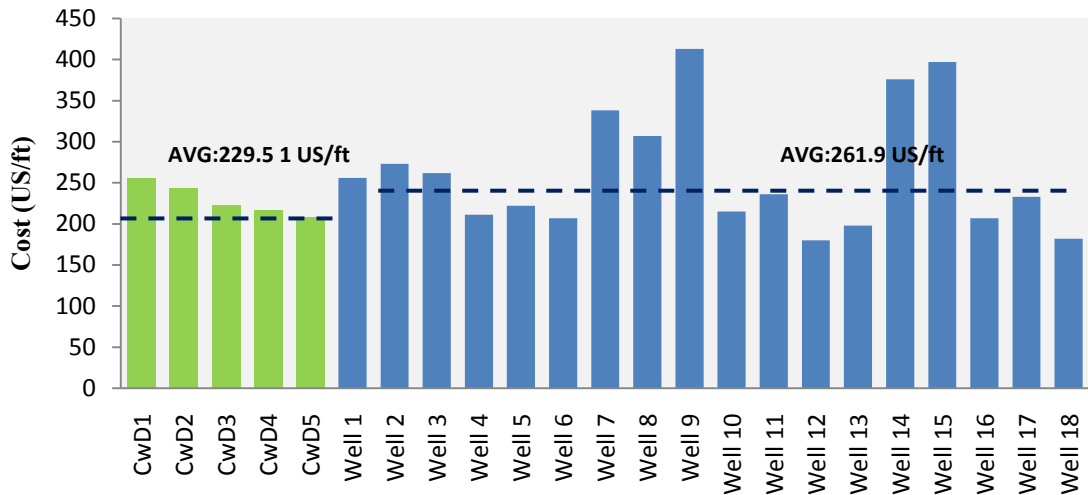


Figure 2.12: Comparison Cost/ft between casing drilling wells and loss circulation wells (Lopez and Bonilla, 2010)

2.4 Limitations of casing while drilling technology

Although this technology is populated with several advantages, it has major restrictions as well. Only few studies objectively analyzed these issues. Some of these limitations are eased with practical solutions and many of them are in the process of being solved through temporary solutions or alternative methods, but the technology needs more development in these areas.

In the operational standpoint, weight on bit applied and pipe rotational speed are restricted. Regular oil field casings are manufactured for the static conditions in wellbore. As they are exposed to the dynamic conditions with the rotational motion; cyclic fatigue, torsion cycles, compressive loads and torsion requirements must be redefined (Galloway, 2004). Usually, the CwD string utilizes no special BHA to provide to WOB; therefore, the lower part of the casing string is in compression.

The most severe limitation comes with the drilling fluid specifications and hydraulics behaviors. A common outcome of this disadvantage is differential sticking. The differential sticking is an issue especially in low pressured permeable zones. The rheological functions of drilling fluid must be designed to withstand this. More importantly, allocating the precise flow rate is on a very critical line. Equivalent

circulating density (ECD) management is surely sensitive. The CwD application utilizes the characteristic narrow annulus to reach high annular fluid velocity and transport cuttings to surface wiping the annulus effectively. The narrow annular clearance puts the annular pressure loss in a vital position. Moderately low flow rates, in comparison to the conventional drilling conditions, satisfy the wellbore cleaning and ECD requirements; however, jetting action, cleaning bit face and cuttings from the bottom hole should be maintained as well (Gupta, 2006). The excessive flow rate leads to fractures in the formation. Although, some authors (Fontenot et al., Watts et al., Karimi et al., and Arlanoglu) mention benefits of having the high pressure profile in annulus on the generation of plastered, strong and high quality seal, it is still uncertain whether the high pressure is a risk or an advantage. Higher ECD is conjectured to initiate small fractures that are readily plugged by plastering effect combined with the stress cage mechanism. On the other hand, it is obvious that excessive ECD can ruin the uniformly shaped filter cake and create fractures. This area needs broad research verified with experiments, field results and modeling.

2.5 Review of hydraulics

It is vital to understand the concept of annular frictional pressure drop and annular velocity due to slight clearance between the hole and the casing. To address these topics, drilling fluid hydraulics is captured in this section. Fluid models, drilling fluid properties and frictional pressure loss calculation studies are discussed.

2.5.1 Drilling fluid rheology

Wellbore hydraulics is a function of the rheology. Rheology, as a study, concerns the deformation and flow of matter. Fluids are subcategorized into the rheological models based on their response in the shear stress and shear rate curves. Shear stress is the equivalent force to maintain a particular type of flow. Shear rate is the ratio of the relative velocity of moving surface to adjacent surface over distance between them. The response of the fluid in a shear stress vs. shear rate curve indicates fluid type; Newtonian fluid and non-Newtonian fluid, rheological properties; viscosity, yield

point and gel strength, and rheological fluid model; Typically, fluids of interest in the oil industry show sensitivity to shear rate rather than time. In order to describe these fluids better, several fluid models have been proposed those are.

- Bingham plastic model
- Power law model and
- Yield power law model

Figure 2.13 addresses Bingham plastic fluid, Power law fluid and Newtonian fluid in a shear rate – shear stress curve. Shear stress and shear rate are calculated using data from Fann VG viscometer and the corresponding values are expressed in secondary axis.

Bingham plastic model

Fluids yield a linear trend in the shear rate vs. shear stress graph. The slope of the line yields plastic viscosity, which is a function of the concentration, size and shape of solids and viscosity of the fluid phase. Separation from the Newtonian fluid is resulted by the stress required to initiate motion. In order to start the fluid moving, a level of stress must be applied and the stress required is called the yield point. Mathematically shear stress (τ), plastic viscosity (μ_p), yield point (τ_y) and effective viscosity (μ_e) are shown as given:

$$\tau = \tau_y + \mu_p \gamma$$

Plastic viscosity and yield point are calculated using reading in Fann VG viscometer.

$$\mu_p = \theta_{600} - \theta_{300}$$

$$\tau_y \left(\frac{lb}{100ft^2} \right) = \theta_{300} - \mu_p$$

Finally effective viscosity of the fluid is given by,

$$\mu_e = \mu_p + \frac{\tau_y}{\gamma}$$

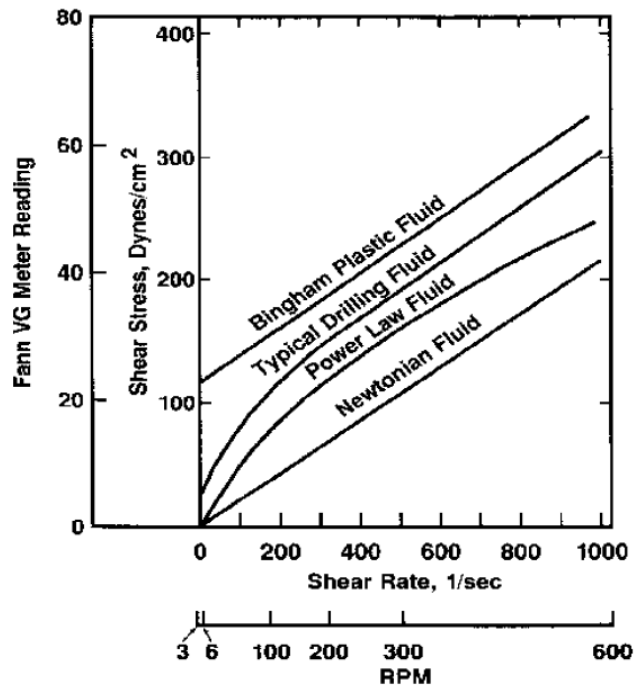


Figure 2.13: Shear stress-Shear rate curve for different fluid types (Taken from Amoco Production Company – Drilling Fluids Manual).

Power law model

Fluids show a parabolic trend in the shear stress vs. shear rate curve. Similar to the trend curve for Newtonian fluids, the curve starts from the origin and based on the value of power law index (n), it reflects a parabolic curve. As n is greater than 1, power law fluid is considered as shear thickening and as n is less than 1, it is shear thinning fluid. Power law index (n), consistency index (K) and apparent viscosity of a power law fluid can be described as given: (Bourgoyne et al. 1986)

$$n = 3.32 \log \left(\frac{\theta_{600}}{\theta_{300}} \right)$$

$$k = \frac{511 \theta_{300}}{511^n}$$

$$\mu = K(\gamma)^{n-1}$$

Yield power law model

This type of fluid is known as Herschel-Bulkley model and closest to the typical drilling fluid. This model is a combination of bingham plastic fluid and power law fluid. Figure 2.17 graphically illustrates the resemblance. A yield stress is required to start flow similar to the behavior in bingham plastic fluids, and the trend of shear stress vs. shear rate curve is parabolic similar to the behavior in power law fluids. The yield power law fluids are mathematically more complex than bingham plastic fluids and power law fluids. Shear stress (τ) and effective viscosity (μ) of the yield power law fluid is given as:

$$\tau = \tau_y + K(\dot{\gamma})^n$$

$$\mu = \frac{\tau_y + k\dot{\gamma}^n}{\dot{\gamma}}$$

2.5.2 Fluid flow and frictional pressure loss analysis for CwD annulus

The behavior of fluid flow field (pressure and velocity) is governed by the fluid rheology, wellbore geometry, and flow rate. In fluid flow applications with slim annular clearance, including CwD, pressure and velocity profiles alter significantly. The alteration occurs in support of high velocity in the annulus and high flowing bottomhole pressure. Fundamentally, the International Well Control Forum (IWCF) expresses the flowing bottomhole pressure as the summation of static bottomhole pressure and annular pressure loss (IWCF, 2006). As the terms in flowing bottomhole expressions are converted from pressure to equivalent mud weight, the equivalent circulating density (ECD) equation is formed

$$ECD = \frac{\Delta P_{fric} + P_h}{D}$$

In this formula, stands for the hydrostatic mud pressure in the annulus, stands for the sum of annulus pressure losses due to friction, and D stands for the depth. The annular pressure losses become significant, because ECD can occasionally be greater than formation fracture gradient. Normally, provided that the mud weight is kept constant, ECD is exposed to limited change, as the frictional pressure drop is not the superior in

hydraulics design for conventional drilling geometries. However, the application of this approach to the CwD circumstances becomes perilous. In the CwD technology, frictional pressure losses predominate. The slimhole drilling applications show similarities to CwD regarding the tight annulus clearance and high annular pressure losses. One of the ways to control the dynamic bottom hole pressure (hence ECD) is through controlling the mud weight. As the mud weight decreases, hydrostatic pressure of the mud column in the annulus decreases. The rheological property of drilling fluid is another gadget to adjust in advance in order to lower the ECD. For instance, lowering plastic viscosity is an option to reduce the ECD. A final caution might be lowering the flow rate, depending on that, lowering velocities in the annulus and reducing the frictional pressure losses. Instead of individual application of any of these three methods; they must be optimized to obtain the best results. This is very crucial for the wellbore cleaning (Karimi et al., 2012).

2.5.3 Annular frictional pressure loss using Narrow Slot Approximation method

Annular flow can be approximated using equations developed for flow through rectangular slots. The slot flow equations are much simpler to use and are reasonably accurate as long as the ratio of the hole radius (r_2) to casing radius (r_1) is greater than 0.3. Figure 2.14 illustrates an annular space that can be represented as a narrow slot having an area (Bourgoyne et al. 1986),

$$A = Wh = \pi(r_2^2 - r_1^2)$$

the flow rate in terms of the mean flow velocity v and solving for the frictional pressure gradient gives $\frac{dp}{dl}$,

$$\frac{dp}{dl} = \frac{12\mu v}{(r_2 - r_1)^2}$$

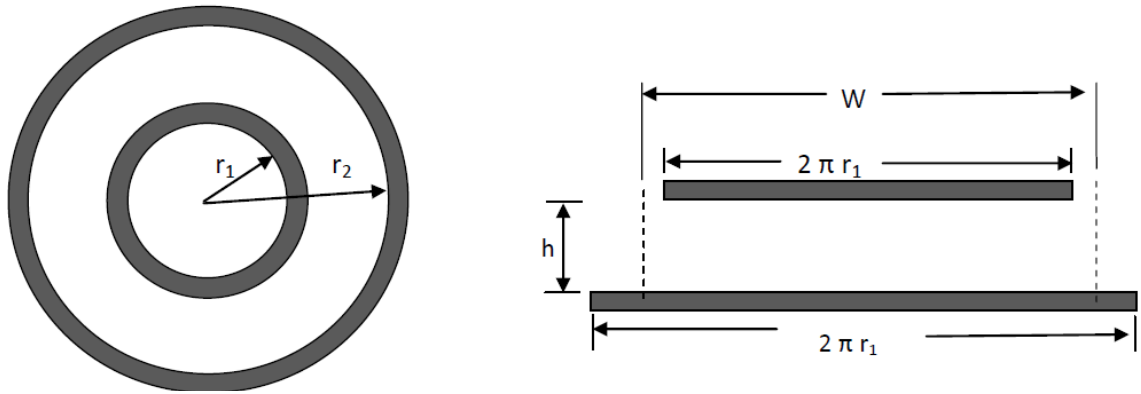


Figure 2.14: Representing the annulus as a slot: (a) annular and (b) equivalent slot

expressing

Determination of shear rate

Knowledge of shear rate present in the well sometimes can lead to improve accuracy in the pressure loss determination. Care can be taken to measure the apparent fluid viscosity at values of shear rates near those present in the well. If this is done, better accuracy sometimes can be achieved using flow equations for Newtonian fluids even if the well fluid does not follow closely the Newtonian model over a wide range of shear rates. The maximum value of shear rate occurs at the pipe walls. Thus the shear stress at the wall where $r = r_w$ is given by,

$$\tau_w = \frac{r_w}{2} \frac{dp}{dl} \quad (\text{Circular pipe})$$

The shear stress for an annulus (slot flow approximation) is given by,

$$\tau_w = \frac{h}{2} \frac{dp}{dl} = \frac{(r_2 - r_1)}{2} \frac{dp}{dl}$$

Finally, in Table 2.1 collection of velocity and pressure loss calculation equations were summarized which are useful for pressure calculations for laminar or turbulent fluid flow under normal circumstances.

Table 2.1: Summary of formulas for annulus frictional pressure drop

		Bingham Plastic	Power Law
Mean Velocity	Pipe	$v = \frac{q}{2.448d^2}$	$v = \frac{q}{2.448d^2}$
	Annulus	$v = \frac{q}{2.448(d_2 - d_1)^2}$	$v = \frac{q}{2.448(d_2 - d_1)^2}$
Frictional Pressure Loss - laminar flow	Pipe	$\frac{dp}{dl} = \frac{\mu p v}{1500d^2} + \frac{\tau_w}{225d}$	$\frac{dp}{dl} = \frac{Kv^n \left(\frac{3 + \frac{1}{n}}{0.416}\right)^n}{144000d^{(1+n)}}$
	Annulus	$\frac{dp}{dl} = \frac{\mu p v}{1000(d_2 - d_1)^2} + \frac{\tau_w}{200(d_2 - d_1)}$	$\frac{dp}{dl} = \frac{Kv^n \left(\frac{2 + \frac{1}{n}}{0.208}\right)^n}{144000(d_2 - d_1)^{(1+n)}}$
Frictional Pressure Loss - Turbulent flow	Pipe	$\frac{dp}{dl} = \frac{\rho f_f v^2}{25.8d}$	$\frac{dp}{dl} = \frac{\rho f_f v^2}{25.8d}$
	Annulus	$\frac{dp}{dl} = \frac{\rho f_f v^2}{25.8(d_2 - d_1)}$	$\frac{dp}{dl} = \frac{\rho f_f v^2}{25.8(d_2 - d_1)}$

CHAPTER 3: METHODOLOGY

3.1 Hydraulic lift phenomenon

Casing drilling process utilizes large diameter casing to drill. The small annulus brings about higher friction which leads to higher equivalent circulating density (ECD) in comparison to conventional drilling. During drilling operations as fluid circulates through large casing and narrow annulus several forces act upwards on the casing that reduces the effective weight on bit Figure 3.1. Major contributing lifting forces are

- a. Drag Forces: Upward frictional forces of fluids on casing wall during CwD operation as fluid passes through narrow annulus.
- b. End Forces: Upward force of fluids as it exits the nozzles and acts upward on the bit face. This force consists of frictional pressure loss through annulus and the hydrostatic pressure required balancing the mud column.

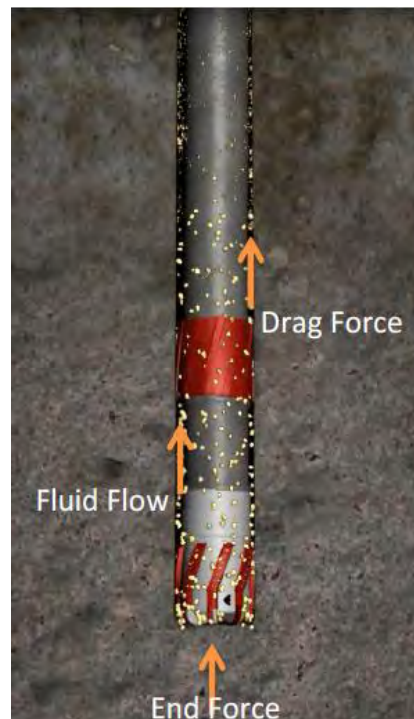


Figure 3.1: Major contributing forces on Hydraulic Lift

3.2 Model description

Hydraulic lift forces involved in a drilling operation are developed for three common well conditions. These well conditions are -

- I. A static conditions in which both well fluid and central pipe string are at rest (Non-circulating)
- II. A circulating operation in which the fluids are being pumped down the central pipe string and up the annulus.(Circulating well)
- III. A tripping operation in which central pipe string is being move up and down through the fluid

To model the overall hydraulic lift circulating well condition is considered. To simplify the model following assumptions are followed

- (i) No effect of casing eccentricity and pipe rotation on pressure loss
- (ii) Sections of open hole are circular in shape and of known diameter
- (iii) Drilling fluid is incompressible
- (iv) Flow is isothermal
- (v) No tool joint effect

Figure 3.2 demonstrates a simple circulating route of drilling fluid while drilling and it is possible to analyze the each section to understand each pressure loss component. In the mud circulation system fluid travels from the still tanks to mud pump, from the pump through the surface equipments to drill string then through drill string to the bit. Afterwards passing the nozzle of the bit fluid moves up through the annular space between the drill string and hole to the surface finally, through contaminant removal equipment back to the mud pit. During mud circulation frictional pressure loss of mud occurs mainly in the surface equipment, inside drill string, in the bit nozzle and through the annulus. When fluid starts to move from mud pump the pressure provided by mud pump is the sum of all pressure loss to circulate the mud continuously. Thus as fluid exits through nozzle the amount of pressure transmitted by the fluid is the sum of frictional pressure drop at annulus and the hydrostatic pressure of the mud column. These pressure requirements have been used to calculate hydraulic lift and can be expressed as-

Hydraulic Lift = Frictional drag force on casing wall (F_1) + End Forces at the bottom (F_2)

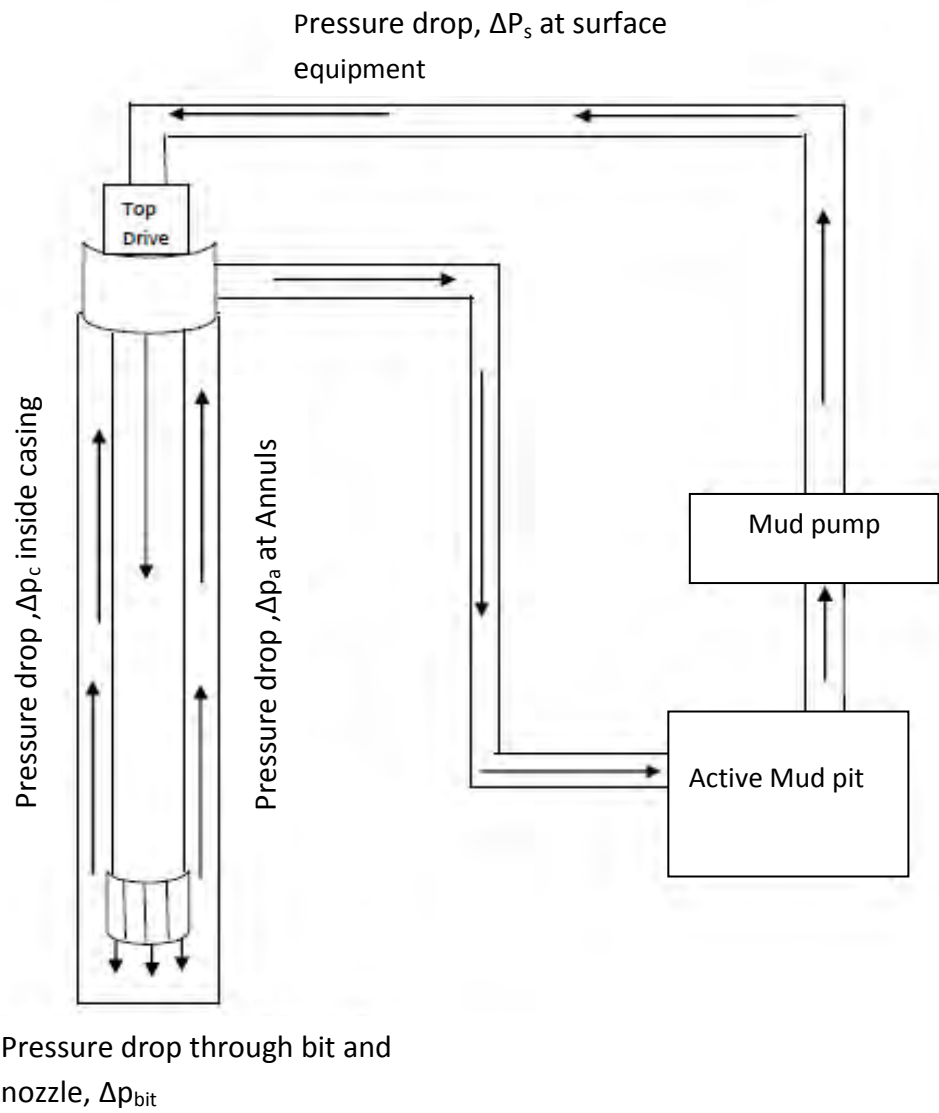


Figure 3.2: Mud circulation system

3.2.1 Model derivation for vertical well with single diameter casing and uniform hole

As fluid circulates through a vertical well single diameter casing two major components comprise the overall hydraulic lift shown in Figure 3.3. To model the overall hydraulic lift these two forces are derived.

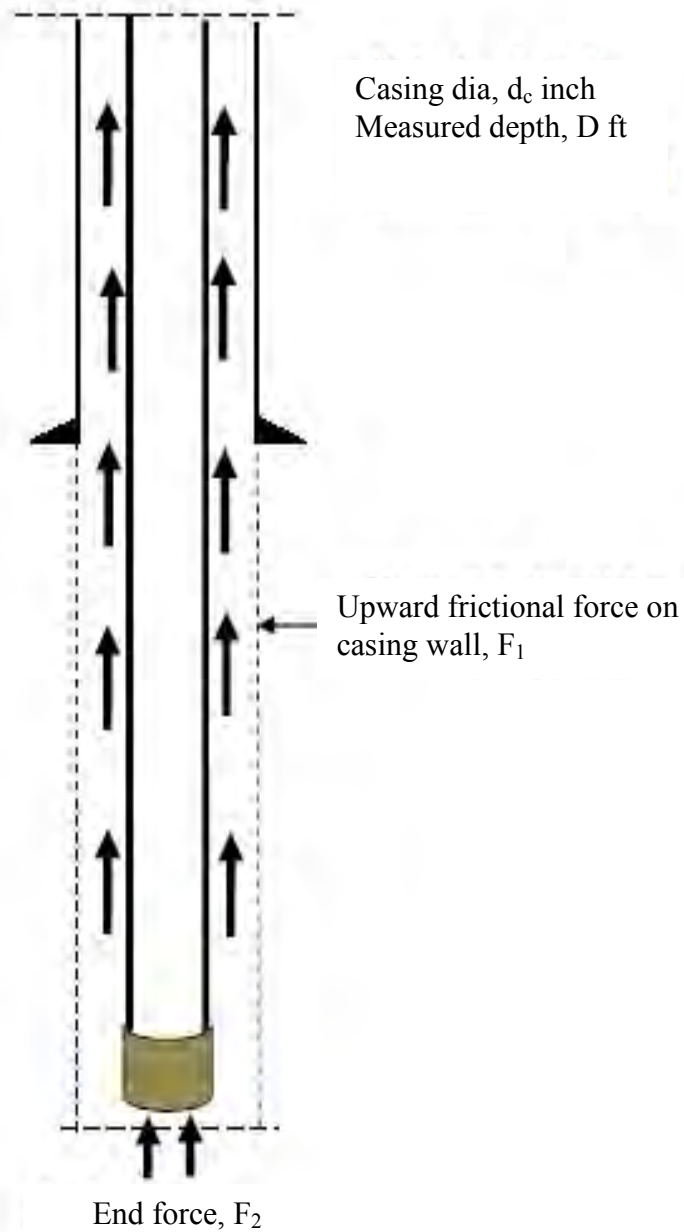


Figure3.3: Contributing forces on hydraulic lift (Vertical Well)

Frictional force on casing wall (F_1)

Frictional pressure on casing wall occurs due to fluid flow through annulus along with cuttings. Effect of cutting is included in the calculation by considering effective mud density. Annular frictional pressure drop can be computed using narrow slot approximation method for various fluid types and flow pattern, (Bourgoyne et al. 1986). Frictional force on casing wall F_1 then can be calculated from shear stress on casing wall.

$$F_1 = \tau_w \times \text{casing area}$$

$$= \left(\frac{d_h - d_c}{4} \right) \times \left(\frac{d_p}{d_l} \right) \times 2\pi \times \frac{d_c}{2} \times D$$

Here, Shear stress on casing wall in psi, $\tau_w = \left(\frac{d_{hA} - d_c}{4} \right) \times \left(\frac{d_p}{d_l} \right)_A$

Annular pressure drop in psi/ft, $\frac{d_p}{d_l} = \frac{\rho f v_a^2}{21.1(d_h - d_c)}$

Annular mud velocity in ft/sec, $v_a = \frac{Q}{2.448 \times (d_h^2 - d_c^2)}$

End forces at the bottom of the casing (F_2)

Amount of pressure contained at the bottom of the casing is the some of annular frictional pressure and the hydrostatic pressure differential between different mud densities. So it can be written as

$$F_2 = \text{Fluid pressure contained at the bottom} \times \text{Area of the bottom of casing}$$

$$= (\text{Annular pressure drop} + \text{Hydrostatic pressure differential at bottom})$$

$$\times \text{Area of the bottom of the casing}$$

$$= \left\{ \frac{d_p}{d_l} + 0.052(\rho_e - \rho_m) \right\} \times D \times \frac{\pi}{4} \times d_c^2$$

Hence, Combining F_1 and F_2 Hydraulic lift can be expressed by following equation,

$$HL = F_1 + F_2$$

$$HL = \frac{\pi}{4} \times D \times \left\{ \left(\frac{d_p}{d_l} \right) \times d_h \times d_c + 0.052 \times d_c^2 (\rho_e - \rho_m) \right\} \quad (3.1)$$

3.2.2 Model derivation for various hole size

Vertical well with varying casing size such as drilling with liner operation where the liner is at the bottom of the string and the end section of the liner pipe extends to the surface figure 3.4. Due to the variation of the hole diameter annular frictional pressure drop also varies for different section. In figure 3.4 upper section is indicated as zone A where hole diameter larger than the lower zone B. To model the overall hydraulic lift for liner drilling frictional drag force for different zone and the end force are derived below.

Annular frictional force on casing wall (F_1)

Following similar procedure annular frictional force can be derived for this case as well

$$F_1 = (\tau_{wA} \times \text{Casing surface area})_{\text{zone A}} + (\tau_{wB} \times \text{Casing surface area})_{\text{zone B}}$$

$$\text{Here, } \tau_{wA} = \left(\frac{d_{hA} - d_c}{4} \right) \times \left(\frac{d_p}{d_l} \right)_A$$

$$\tau_{wB} = \left(\frac{d_{hB} - d_c}{4} \right) \times \left(\frac{d_p}{d_l} \right)_B$$

$$F_1 =$$

$$\left\{ \left(\frac{d_{hA} - d_c}{4} \right) \times \left(\frac{d_p}{d_l} \right)_A \times 2\pi \times \frac{d_c}{2} \times D_A \right\} + \left\{ \left(\frac{d_{hB} - d_c}{4} \right) \times \left(\frac{d_p}{d_l} \right)_B \times 2\pi \times \frac{d_c}{2} \times (D - D_A) \right\}$$

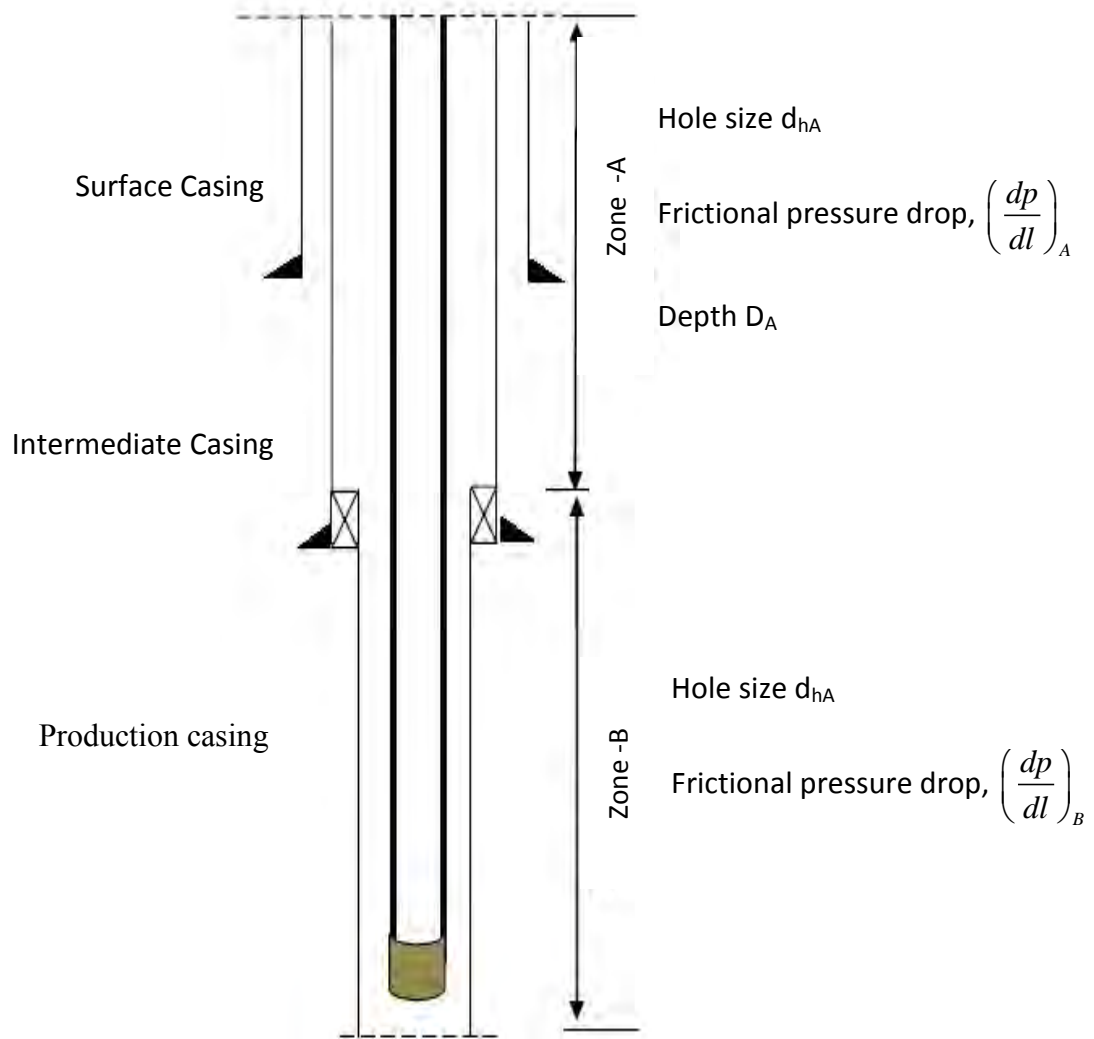


Figure 3.4: Schematic of a typical liner drilling wellbore

End forces at the bottom of the Casing (F_2)

Following the similar procedure end force can be derived as

$$\begin{aligned}
 F_2 &= \text{Fluid pressure exists at the bottom} \times \text{Area of the bottom of casing} \\
 &\quad \text{face} \\
 &= (\text{Annular pressure loss} + \text{Hydrostatic pressure at bottom}) \times \text{Area}
 \end{aligned}$$

Annular Frictional Pressure loss for Zone A,

$$= \left(\frac{d_p}{d_l} \right)_A \times D_A$$

Annular Frictional Pressure loss for Zone B,

$$= \left(\frac{d_p}{d_l} \right)_B \times (D - D_A)$$

End Force, $F_2 =$

$$\left[\left\{ \left(\frac{d_p}{d_l} \right)_A \times D_A \right\} + \left\{ \left(\frac{d_p}{d_l} \right)_B \times (D - D_A) \right\} + \left\{ 0.052 \times d_c^2 (\rho_e - \rho_m) \times D \right\} \right] \times \frac{\pi}{4} \times d_c^2$$

Similarly, combining both F_1 and F_2 overall hydraulic lift can be expressed as,

$$HL = F_1 + F_2$$

$$HL = \left\{ \left(\frac{d_{hA} - d_c}{4} \right) \times \left(\frac{d_p}{d_l} \right)_A \times 2\pi \times \frac{d_c}{2} \times D_A \right\} + \left\{ \left(\frac{d_{hB} - d_c}{4} \right) \times \left(\frac{d_p}{d_l} \right)_B \times 2\pi \times \frac{d_c}{2} \times (D - D_A) \right\} \\ + \left[\left\{ \left(\frac{d_p}{d_l} \right)_A \times D_A \right\} + \left\{ \left(\frac{d_p}{d_l} \right)_B \times (D - D_A) \right\} + \left\{ 0.052 \times d_c^2 (\rho_e - \rho_m) \times D \right\} \right] \times \frac{\pi}{4} \times d_c^2 \quad (3.2)$$

3.2.3 Model for Inclined well operation

To develop the hydraulic lift model for a deviated well annular frictional force on casing wall for the vertical section and inclined section are derived with measured depth. Only vertical component of the force that created in the inclined section including end force is considered for the hydraulic lift figure 3.5. Therefore the overall hydraulic lift for inclined well will be,

Total Hydraulic Lift ,

$$= [\text{Frictional Drag force, } F_1]_{\text{vertical}} + (\text{Frictional force } F_2 + \text{End force}$$

$$F_3)_{\text{inclined}} \text{Cos}\theta$$

$$= F_1 + (F_2 + F_3) \times \text{Cos}\theta$$

Here, frictional forces and end force can be calculated using conventional formulas as previously done.

Annular Frictional Force on casing wall (F_1)

For vertical section up to kick off depth, frictional force, F_1 on casing wall can be derived similarly.

$$F_1 = \left(\frac{d_h - d_c}{4} \right) \times \left(\frac{d_p}{d_l} \right) \times 2\pi \times \frac{d_c}{2} \times D_{kickoff}$$

For the inclined section frictional force on casing wall,

$$F_2 = \left(\frac{d_h - d_c}{4} \right) \times \left(\frac{d_p}{d_l} \right) \times 2\pi \times \frac{d_c}{2} \times D_{MD}$$

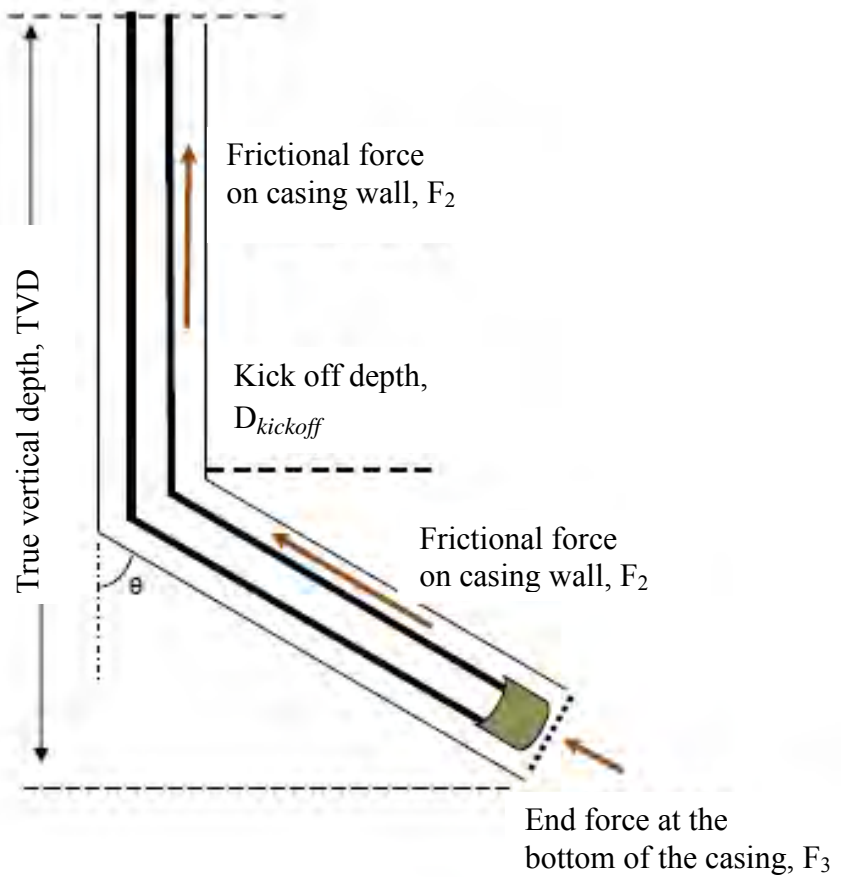


Figure3.5: Contributing forces on hydraulic lift in inclined well

End force at the bottom of the casing F_3 ,

Force acting on the bit face can be derived by similar way. However, to calculate the overall lifting force only the vertical component of the forces are considered.

$$F_3 = \left\{ \frac{d_p}{d_l} + 0.052(\rho_e - \rho_m) \right\} \times D_{TVD} \times \frac{\pi}{4} \times d_c^2$$

Therefore, combining all the forces ,

$$\text{Total Hydraulic Lift} = F_1 + (F_2 + F_3) \cos \theta$$

$$= \left\{ \left(\frac{d_h - d_c}{4} \right) \times \left(\frac{d_p}{d_l} \right) \times 2\pi \times \frac{d_c}{2} \times D_{kickoff} \right\} + \quad (3.3)$$

$$\left[\left(\frac{d_h - d_c}{4} \right) \times \left(\frac{d_p}{d_l} \right) \times 2\pi \times \frac{d_c}{2} \times D_{MD} + \left\{ \frac{d_p}{d_l} + 0.052(\rho_e - \rho_m) \right\} \times D_{TVD} \times \frac{\pi}{4} \times d_c^2 \right] \cos \theta$$

3.2.4 Field measuring procedure of hydraulic lift

To measure the overall hydraulic lift at the field following steps are follows.

- a. Record hookload with bit off bottom, pumps off, and rotating the casing slowly.
- b. Engage mud pump(s) and bring flow rate up to drilling speed and record hookload.
- c. Difference in hookload between having pumps on and off is the hydraulic lift.
- d. Bring Zero WOB
- e. Begin drilling.

CHAPTER 4: CASE STUDIES

In this chapter the results from hydraulic lift are discussed for a vertical well. Effect of different parameters on hydraulic lift is analyzed for drilling hydraulic optimization. To verify the derived hydraulic lift model, a vertical section of a well has been taken into consideration for the calculation purpose. Hydraulic lift is then measured by theoretical model for different flow rates and measured depth. Calculated values obtained from this model are compared with values measured using field method. The comparisons and analysis in this study helped to recognize the well bore condition during drilling.

4.1 Background of the field

In 2015 Weatherford operated a drilling operation using their casing drilling technology in United States. An Operator X Energy contacted Weatherford to determine if DwC™ technology could enable drilling their 7 inch surface casing to mitigate hole stability problems seen in offset wells. After reviewing available offset drilling reports and mud logs, it was recommended that a 7 inch × 8-1/2 inch Defyer 5513™ bit to be used to drill from 8,700 ft to 9,204 ft MD. A 20 inch conductor casing string had previously been set and cemented at ±110 ft MD, and a 9-5/8 inch casing string had been set and cemented at 1,700 ft. The 8-3/4 inch open hole was drilled from 1,700 ft to 8,700 ft prior to the DwC™ operation.

During the 04-05 February, 2015 the 7 inch× 8-1/2 inch casing was drilled from 8,700 ft MD to 9,204 ft MD, and cemented Figure 4.1. To rotate the casing, Frank's CRT (Evolution 4000) was used, which limited the torque in the DwC™ operation. While drilling, the torque and WOB parameters were moving up and down. High torque was seen before lubricating additive was pumped down hole. In this operation during the first two joints of casing, a consistent drilling pattern could not be established. However, after cleaning the bit and BHA with walnut sweeps w/soap, the ROP increased. The average on bottom ROP for this DwC™ job was 20.8ft/hr. Summary of the casing drilling operating parameters are presented in Table 4.1- 4.3

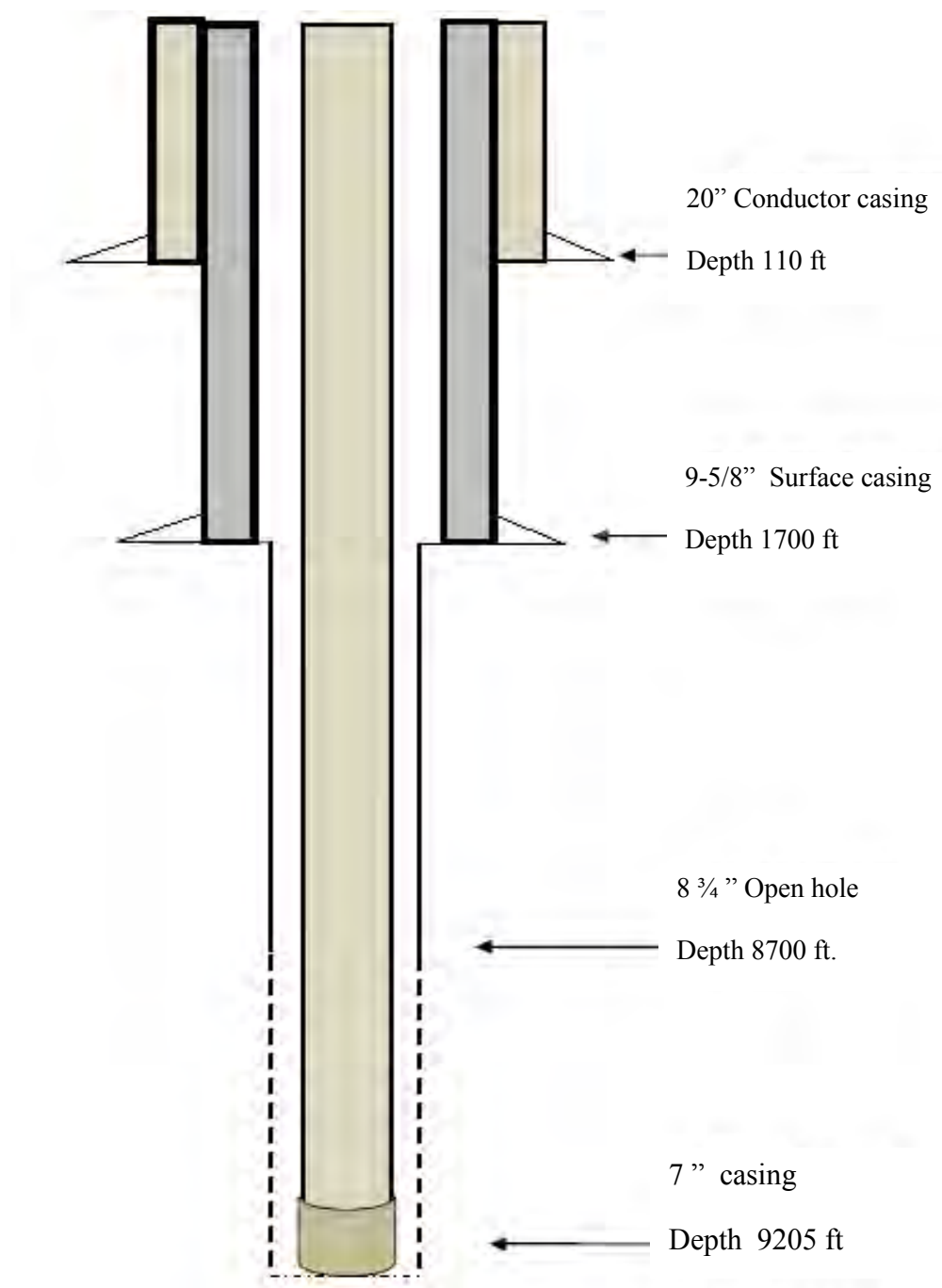


Figure 4.1: Wellbore geometry of the well to be analyzed

Table 4.1: Well parameters (Source: Weatherford International)

Well INFORMATION	
Rig Type	Land Rig
Job Type	DwC
Hole Size	8.5 inch
Last Casing	9-5/8" J-55
Rock Type	Sand/shale
EQUIPMENT	
Defyer TM Size	8.5
Casing Category	Intermediate
Casing Size	7.00 inch
Casing Weight	29 lbf/ft
Casing Grade	P-110 EC
Casing Connection	VAM DwC
Nozzle Qty	7
Nozzle Size [1/32"]	14

Table 4.2: Mud properties (Source: Weatherford International)

MUD PROPERTIES	
Mud Type	LSND
Mud Weight	8.8 lbm/gal
PV	6
YP	10

Table 4.3: Summary of the casing drilling operation. (Source: Weatherford International)

Depth In	8700 ft
Depth Out	9204 ft
Total Distance	504 ft
WOB	4 - 20 kips
RPM	40 – 100
Flow Rate	250 – 350 gpm

4.2 Factors affecting HL

In this study fluid hydraulic principle is used to develop the HL mode. Annular frictional pressure drop and hydrostatic pressure differential in the mud column are used as a function of total lifting force. The parameters that have effect on these forces will also change the overall HL. Frictional pressure drop depends on the pump flow rate and annular velocity while hydrostatic pressure differential depends on the mud density and cuttings concentration. Effect of these parameter is discussed in this section.

4.2.1 Effect of mud flow rate

According to the fluid hydraulics theory velocity is directly proportional to flow rate. So increment of flow rate will increase the velocity and frictional pressure drop as well. To show the effect a typical well is considered where all the properties remain constant and by changing the flow rate the variation of HL can be can be visualize. Following parameter are used for the calculation purpose Table 4.4.

Table 4.4: Different flow rates used to show the effect

Mud Type	Flow Rate gpm
Mud A	250
Mud A	300
Mud A	350

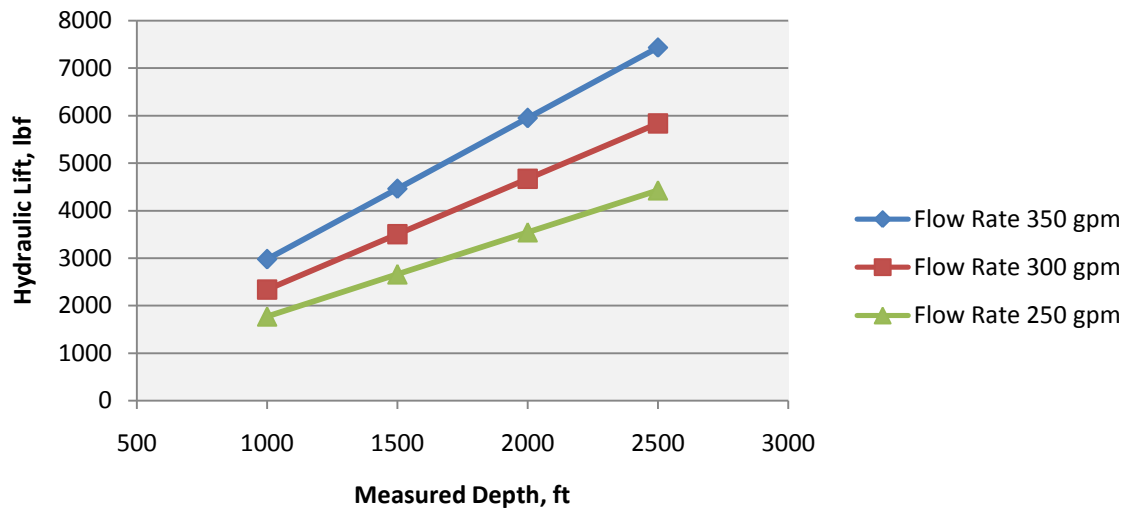


Figure 4.2 Effect of flow rate on HL

Figure 4.2 illustrates the change of HL with different flow rates. It can be figure out that as flow rate increased from 250 gpm to 350 gpm HL also rise. Another feature is that the variation of the HL enhanced significantly with the measured depth.

4.2.2 Effect of borehole size

Fluid velocity is inversely proportional to the flowing area of the annulus. With the reduction of flowing area fluid velocity rises and cause the increment of frictional pressure drop. To illustrate the effect of hole size for three different type of hole diameters are taken considering other parameters constant for the calculation Table 4.5. HL increase significantly with the reduction of annular space according to the Figure 4.3.

Table 4.5: Well bore parameters used to show the effect of hole size

Mud Type	Casing Size, in	Hole Size, in
Mud A	7	8.75
Mud A	7	8.50
Mud A	7	8.25

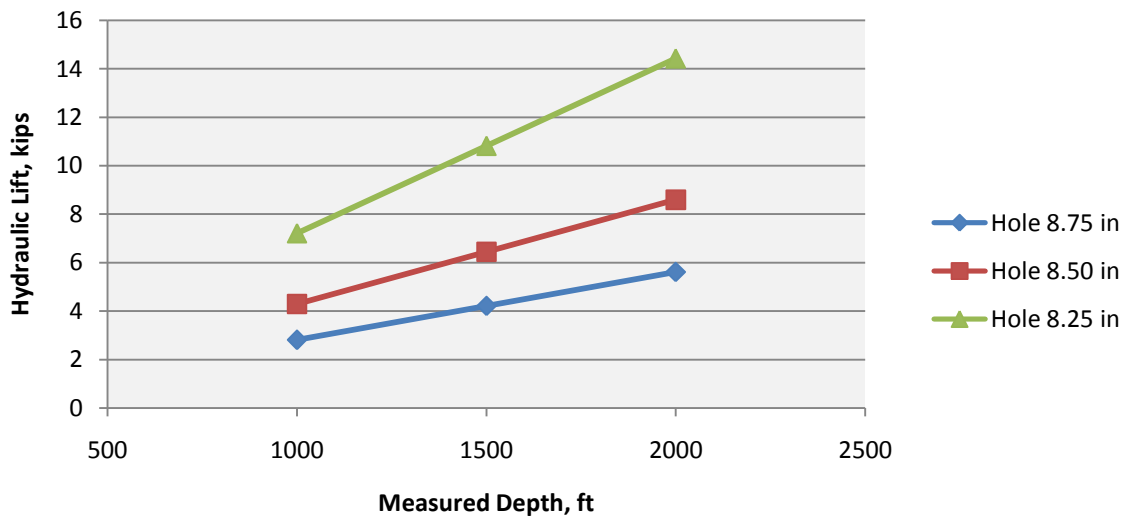


Figure 4.3 Effect of hole size on HL

4.2.3 Effect of cuttings concentration

Effect of cuttings on overall HL is added as effective mud density in the calculation. Hydrostatic pressure differential used in the model will vary with the effective mud density. Figure 4.4 shows that HL increased to some extent with the cuttings concentration but with the distance variation will enhance. parameter used for this calculation is tabulated in Table 4.6.

Table 4.6: Properties used to show the effect of cuttings

Mud Type	Casing Size, in	Hole Size, in	Cuttings Concentration
Mud A	7	8.875	0.0025
Mud A	7	8.875	0.0075
Mud A	7	8.875	0.01

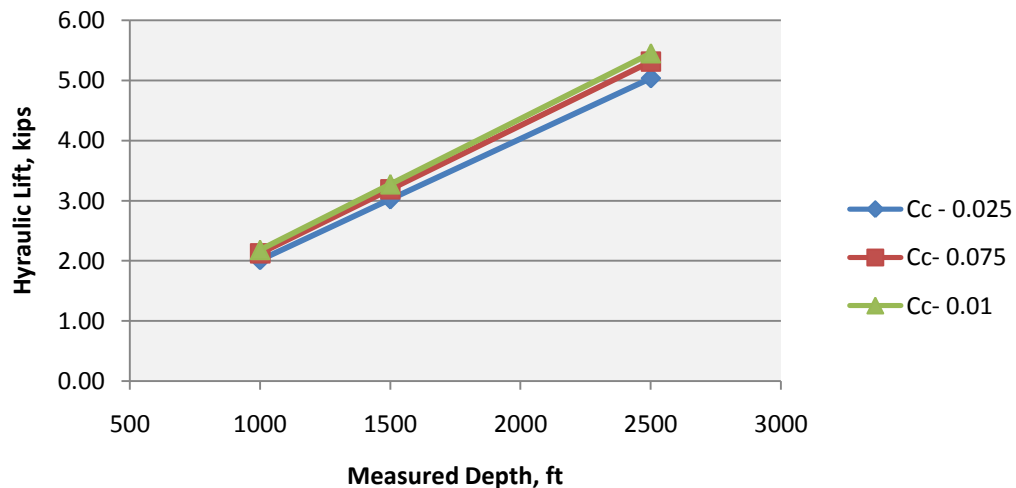


Figure 4.4: Effect of cuttings concentration on HL

4.2.4 Criteria to evaluate the predicted and measured HL

In this study HL is modeled as a tool to examine the wellbore condition. The principle used to monitor the well is that frictional pressure drop increases with fluid velocity and fluid velocity is proportional to the flowing area. While HL is modeled as a function of annular frictional pressure drop, change of this pressure drop will reflect on overall HL. Thus, any flow restriction will essentially increase the HL.. During the field procedure hook loads are measured with bit off bottom condition while using the model HL is measured considering effective mud density including the effect of cuttings. Therefore, following criteria can be used in comparisons of field measured value and predicted value.

- $HL_{\text{Measured}} > HL_{\text{Predicted}}$ poor well bore condition
- $HL_{\text{Measured}} \leq HL_{\text{Predicted}}$ improved well bore condition

4.3 Result analysis of the predicted and field measured value

During DwC operation after 8700 ft casing was run to drill 504 ft with different flow rate to reach the target depth 9204 ft. From the report of the well it has been found that the drilling was inconsistent with the reduced rate of penetration for the first two joints and it was up to depth 8770 ft. To increase the rate of penetration and hole cleaning efficiency the drill bit and bottom hole assembly was cleaned. Thus, To calculated the HL the operation is divided into two stages. Flow rates used in different interval depth is shown in Table 4.7.

Table 4.7: Flow rates at different interval depth.

	Depth, ft	Flow Rate, gpm
Before Cleaning BHA	8700 – 8715	269
	8715 – 8750	293
	8750 – 8765	332
After Cleaning BHA	8765 – 9180	318
	9180 -9204	342

In this study total lifting force is calculated for three different cases. At first HL is measured at 8715 ft with pump flow rate 293 gpm. Then it is measured at interval 8775- 9180 ft before start drilling with flow rate 318 gpm. Finally at 9190 -9205 ft while the flow rate was 342 gpm. The detail calculations of the cuttings concentration and annular frictional pressure drop are described in the appendix section.

Model selection

As there is variation in the hole size model derived for the vertical well with various hole size is used to calculate the HL for the mentioned well. The well is divided into two zones Figure 4.5. From surface to 1700 ft depth where the 9-5/8 casing is seated is termed zone A and rest of the well from 1700 ft is zone-B. Hole size is 8.835 inch and 8.5 inch respectively for zone A and zone B.

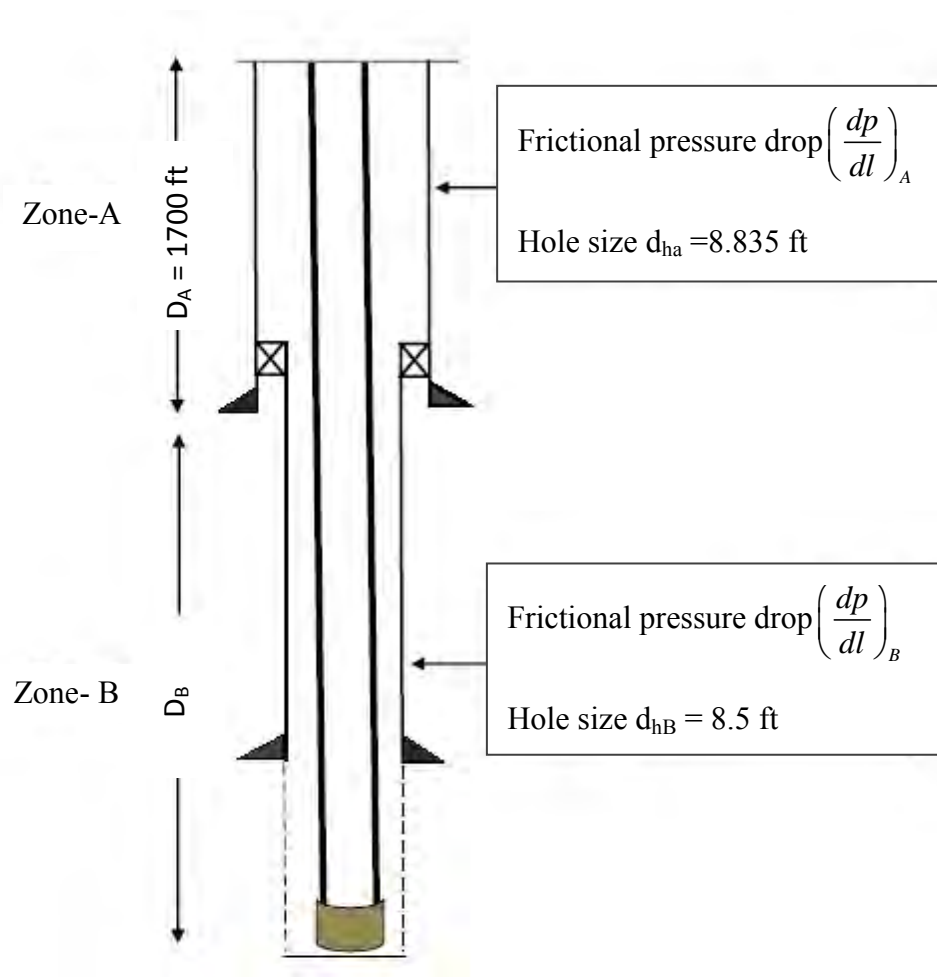


Figure 4.5: Well bore geometry used in HL measurement

4.3.1 Study of HL using the model at depth 8715-8750 ft- Section I

The operation was started with flow rate 269 gpm and after drilling a certain distance flow rate changed to 293 gpm. HL is predicted for the interval of 8715-8735 ft with the pump output 293 gpm.

Prediction of HL using the model – Section I

In prediction of HL calculation is performed using equation (3.2). Frictional pressure drops are 0.032 psi/ft and 0.06 psi/ft respectively for zone A and zone B from Appendix A and Table A. Parameters used in the computation are listed in Table 4.8.

$$\begin{aligned}
 \text{HL} = & \left\{ \left(\frac{d_{hA} - d_c}{4} \right) \times \left(\frac{d_p}{d_l} \right)_A \times 2\pi \times \frac{d_c}{2} \times D_A \right\} + \left\{ \left(\frac{d_{hB} - d_c}{4} \right) \times \left(\frac{d_p}{d_l} \right)_B \times 2\pi \times \frac{d_c}{2} \times (D - D_A) \right\} \\
 & + \left[\left\{ \left(\frac{d_p}{d_l} \right)_A \times D_A \right\} + \left\{ \left(\frac{d_p}{d_l} \right)_B \times (D - D_A) \right\} + \left\{ 0.052 \times d_c^2 (\rho_e - \rho_m) \times D \right\} \right] \times \frac{\pi}{4} \times d_c^2
 \end{aligned}$$

Table 4.8: Parameter used in the model for flow rate 293 gpm

Casing size	7 inch
Hole size zone A	8.835 ft
Hole siz zone B	8.5 ft
Frictional pressure drop zone-A, $\left(\frac{dp}{dl} \right)_A$	0.032 psi/ft
Frictional pressure drop zone- B, $\left(\frac{dp}{dl} \right)_A$	0.06 psi/ft
Effective mud density, ρ_e ,	8.84 lbm/gal

The results obtained from this model are tabulated in Table 4.9. Graphical representation of hydraulic lift with measured depth indicates that overall HL increases with depth linearly if each parameter remains constant with depth Figure 4.6. This upward trend is due to the fact that, HL model is derived as a function of frictional pressure drop and hydrostatic pressure differential of the annulus mud column which rises with depth.

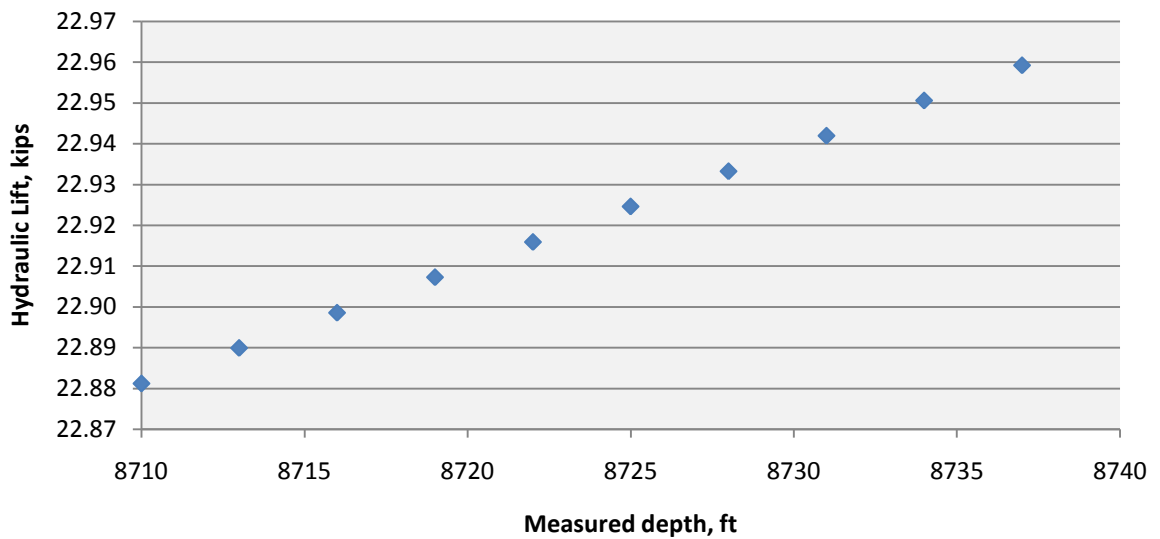


Figure 4.6: HL vs Measured depth at flow rate 293 gpm

Table 4.9: HL calculation for 8710- 8735 ft

Measured Depth.ft	Depth from 9-5/8 casing,ft	Clean Mud density, lbm/gal	Cuttings concentration	Effective mud density, lbm/gal	Plastic viscosity	Yield Point	Casing dia, inch	Hole dia, inch	Constant Flow rate, gpm	Annular Velocity, ft/s	Hedstrom number for Bingham Plastic model	Reynolds number	Friction factor	Anulur frictional pressure drop, psi/ft	Total frictional pressure drop, psi/ft	Drag Force due to annular flow, lbf	Upward force at the bottom due to annular pressure drop, lbf	Force due to hydrostatic pressure differntial in mud column, lbf	End force, lbf	Total HL lift, Kips
D	D _A	ρ_m	Cc	ρ_e	pv	YP	dc	dh	Q	Va	He	Nre	ff	dp/dl		F ₁ , lb	F _{2a} · Lbf	F _{2b} , lbf	F ₂ = (F _{2a} +F _{2b})	(F ₁ + F ₂),
1700	0	8.8	0.0029	8.84	6	10	7	8.84	293	4.12	203306	8392	0.008	0.032	0.03	546				
8710	7010	8.8	0.0029	8.84	6	10	7	8.5	293	5.15	135850	8573	0.008	0.060	0.055	3495	18273	624	18898	22.95
8713	7013	8.8	0.0029	8.84	6	10	7	8.5	293	5.15	135850	8573	0.008	0.060	0.055	3497	18280	625	18905	22.96
8716	7016	8.8	0.0029	8.84	6	10	7	8.5	293	5.15	135850	8573	0.008	0.060	0.055	3498	18287	625	18912	22.97
8719	7019	8.8	0.0029	8.84	6	10	7	8.5	293	5.15	135850	8573	0.008	0.060	0.055	3500	18294	625	18919	22.97
8722	7022	8.8	0.0029	8.84	6	10	7	8.5	293	5.15	135850	8573	0.008	0.060	0.055	3501	18301	625	18927	22.98
8725	7025	8.8	0.0029	8.84	6	10	7	8.5	293	5.15	135850	8573	0.008	0.060	0.055	3503	18308	625	18934	22.99
8728	7028	8.8	0.0029	8.84	6	10	7	8.5	293	5.15	135850	8573	0.008	0.060	0.055	3504	18315	626	18941	23.00
8731	7031	8.8	0.0029	8.84	6	10	7	8.5	293	5.15	135850	8573	0.008	0.060	0.055	3506	18322	626	18948	23.01
8734	7034	8.8	0.0029	8.84	6	10	7	8.5	293	5.15	135850	8573	0.008	0.060	0.055	3507	18329	626	18955	23.02

Measurement of HL using field procedure – Section I

In this case HL is measured for certain depths within the distance between 8710 ft to 8735 ft. The pump was run with 293 gpm throughout the distance while the rotary rpm was about 60-80. Results obtained for these flow rates are tabulated in Table 4.10.

Table 4.10: Field measurement of HL at depth 8710-8735ft and flow rate 293gpm

Timestamp	Hole Depth	Hook Load	Rotary RPM	Total Pump Output	Bit Depth	Hook Load	Hook Load pump off	HL
2015-02-04T12:51:00	8716.4	302.9	60.9	293.7	8710.5	302.9	330.26	27.4
2015-02-04T12:51:10	8716.4	302.2	60.9	293.7	8711.2	302.2	330.28	28.1
2015-02-04T12:51:20	8716.4	302.1	60.8	293.7	8711.8	302.1	330.29	28.2
2015-02-04T12:51:30	8716.4	302.3	60.8	293.7	8712.5	302.3	330.31	28.0
2015-02-04T12:51:40	8716.4	302.5	60.8	293.7	8713.2	302.5	330.32	27.8
2015-02-04T12:51:50	8716.4	302.3	60.8	293.7	8713.9	302.3	330.34	28.0
2015-02-04T14:43:40	8733	310	81.5	293.7	8730.2	310	330.74	20.7
2015-02-04T14:43:50	8733	309.1	81.1	293.7	8730.7	309.1	330.76	21.7
2015-02-04T14:44:00	8733	307.9	80.1	293.7	8730.9	307.9	330.76	22.9
2015-02-04T14:44:10	8733	306.8	80	293.7	8731.4	306.8	330.77	24.0
2015-02-04T15:17:40	8734.8	303.6	60.8	293.7	8734	303.6	330.84	27.2
2015-02-04T15:17:50	8734.8	306.2	60.8	293.7	8734.1	306.2	330.84	24.6
2015-02-04T15:18:00	8734.8	308.4	60.8	293.7	8734.2	308.4	330.84	22.4
2015-02-04T15:18:10	8734.8	307.1	60.7	293.7	8734.3	307.1	330.84	23.7
2015-02-04T15:18:20	8734.8	305.1	60.8	293.7	8734.4	305.1	330.85	25.7

Comparison of field measured value and calculated value

To compare the predicted values and field measured values both are plotted with respect to measured depth. Figure 4.7 shows within the interval between 8710 ft to 8735 ft using field measuring procedure HL lift determined only for certain bit depths. All the way through the distance predicted values using the model shows steady trend with HL around 23 kips. Field measured values on the other hand is 28 kips for the distance 8710 ft -8715 ft and around 25 kips for 8730ft to 8735 ft. Although few field values are lower near 8730 ft but throughout the interval most of the field values are higher than the predicted values.

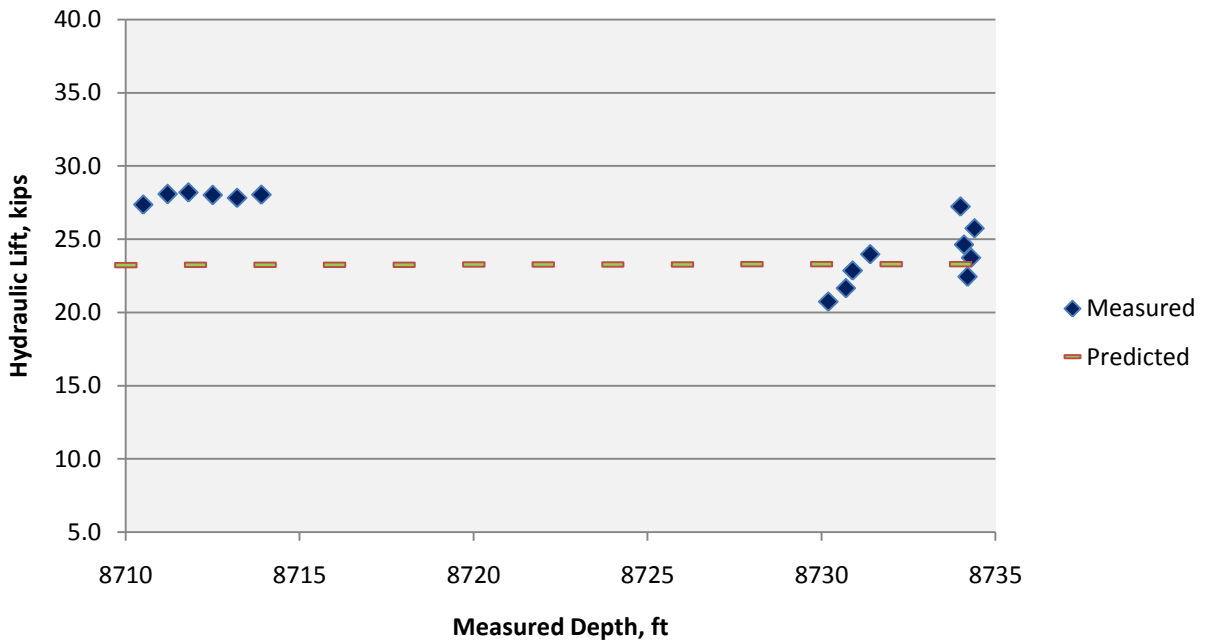


Figure 4.7: Comparison between measured HL and predicted HL for depth 8710ft – 8735 ft with flow rate 293 gpm

Analysis of the study

The calculated result for flow rate 293 gpm within the distance 8710 ft to 8735 ft is compared with the real field data. Calculated value is found significantly lower than the real field measured value ignoring the outliers. This variation occurred due to formation of packing in the wellbore. While hole cleaning is not sufficient packing tend to form which reduced the flowing area of the annulus and causes the increment of frictional pressure drop. Using the model calculation is performed considering uniform annulus. However, the field report and observation implies incompatible drilling operation in terms of poor hole cleaning and lower ROP for first two joints up to nearly 8780 ft. As a result the operator had to clean the BHA and pump down additives in order to improve the wellbore condition. So it can be relates that the inconsistency of drilling was due to poor well bore condition which also reflected from the comparison of HL. Therefore, derived HL model can be considered valid for this case.

4.3.2 Study of HL using the model at depth 8770-9180 ft- Section II

During the operation after drilling first two joints to depth nearly 8780 ft it has been observed that ROP and hole cleaning was insignificant. To mitigate this problem few remedial action was taken in to the well bore. After cleaning the BHA and bit drilling started again from 8780 ft with increased flow rate of 318 gpm.

Prediction of HL using the model – Section II

At this interval drilling operation was performed with flow rate 318 gpm. Similarly using equation (3.2) HL is measured. Table 4.11 shows the parameter used in the equation from Table A. Graphical representation of HL for this distance is presented in Figure 4.8 and calculated values are shown in Table 4.12. Figure 4.8 illustrates that overall HL increases with depth linearly if each parameter remains constant with depth. This upward trend is due to the fact that, HL model is derived as a function of frictional pressure drop and hydrostatic pressure differential of the annulus mud column which rises with depth.

Table 4.11: Parameter used in the model for flow rate 318 gpm

Frictional pressure drop zone-A, $\left(\frac{dp}{dl}\right)_A$	0.032 psi/ft
Frictional pressure drop zone- B, $\left(\frac{dp}{dl}\right)_B$	0.07 psi/ft
Effective mud density, ρ_e ,	8.83 lbm/gal

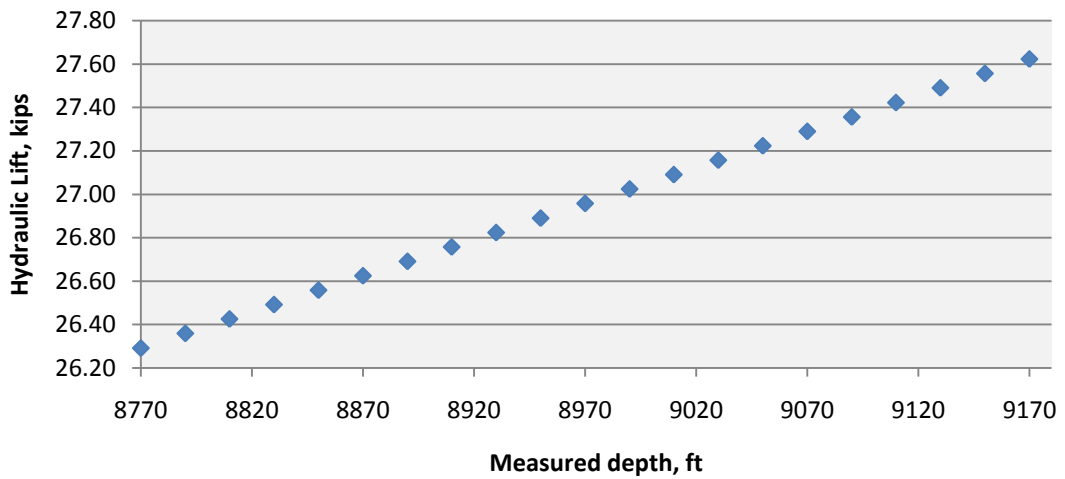


Figure 4.8: HL vs measured depth at flow rate 318 gpm

Table 4.12: HL calculation for 8770-9180 ft

Measured Depth.ft	Depth from 9-5/8 casing,ft	Clean Mud density, lbm/gal	Cuttings concentration	Effective mud density, lbm/gal	Plastic viscosity	Yield Point	Casing dia, inch	Hole dia, inch	Constant Flow rate, gpm	Annular Velocity, ft/s	Hedstrom number for Bingham Plastic model	Reynolds number	Friction factor	Anular frictional pressure drop, psi/ft	Total frictional pressure drop, psi/ft	Drag Force due to annular flow, lbf	Upward force at the bottom due to annular pressure drop, lbf	Force due to hydrostatic pressure differential in mud column, lbf	End force, lbf	Total HL lift, Kips
D	D _A	ρ _m	C _c	ρ _e	p _v	YP	dc	dh	Q	V _a	He	N _{re}	ff	dp/dl		F ₁ , lb	F _{2a} . Lbf	F _{2b} , lbf	F ₂ = (F _{2a} +F _{2b})	(F ₁ + F ₂),
1700	0	8.8	0.0026	8.83	6	10	7	8.84	318	4.47	203306	9108	0.008	0.037	0.03	630				
8770	7070	8.8	0.0026	8.83	6	10	7	8.5	318	5.59	135850	9305	0.008	0.070	0.062	4068	20948	561	21509	26.05
8820	7120	8.8	0.0026	8.83	6	10	7	8.5	318	5.59	135850	9305	0.008	0.070	0.062	4097	21082	565	21646	26.21
8870	7170	8.8	0.0026	8.83	6	10	7	8.5	318	5.59	135850	9305	0.008	0.070	0.062	4126	21216	568	21784	26.38
8920	7220	8.8	0.0026	8.83	6	10	7	8.5	318	5.59	135850	9305	0.008	0.070	0.062	4155	21350	571	21921	26.55
8970	7270	8.8	0.0026	8.83	6	10	7	8.5	318	5.59	135850	9305	0.008	0.070	0.062	4183	21485	574	22059	26.71
9020	7320	8.8	0.0026	8.83	6	10	7	8.5	318	5.59	135850	9305	0.008	0.070	0.062	4212	21619	577	22196	26.88
9070	7370	8.8	0.0026	8.83	6	10	7	8.5	318	5.59	135850	9305	0.008	0.070	0.062	4241	21753	581	22334	27.04
9120	7420	8.8	0.0026	8.83	6	10	7	8.5	318	5.59	135850	9305	0.008	0.070	0.062	4270	21887	584	22471	27.21
9170	7470	8.8	0.0026	8.83	6	10	7	8.5	318	5.59	135850	9305	0.008	0.070	0.062	4299	22022	587	22609	27.38

Measurement of HL using field procedure – Section II

Following similar procedure results obtained for interval 8770 ft to 9180 ft with flow rate 318 gpm are listed in Table 4.13.

Table 4.13: Field measurement of HL at depth 8770-9180 ft and flow rate 318gpm

Hole Depth	Rotary RPM	Total Pump Output	Weight on Bit	Bit Depth	Hook Load	Hook load pump off	HL
8775.9	65.5	318	0	8773	307.9	331.8	23.9
8775.9	65.6	318	0	8773	307.5	331.8	24.3
8903.4	80.2	318	0	8899	304.8	334.9	30.1
8903.4	80.1	318	0	8899	304.8	334.9	30.1
8903.4	80	318	0	8901	304.1	334.9	30.8
8947.9	66.5	318	2.6	8943.5	319.6	336.0	16.4
8947.9	66.2	318	1.3	8945.1	315.8	336.0	20.2
8989.3	80.4	318	0	8987.3	319.4	337.1	17.7
8989.3	80.3	318	0	8987.3	312.9	337.1	24.2
9042.6	80.1	318	0	9034.8	311.1	338.2	27.1
9042.6	80.1	318	0	9034.8	310.1	338.2	28.1
9042.6	80	318	0	9034.8	310.3	338.2	27.9
9042.6	80.2	318	0	9035.8	313.3	338.3	25.0
9042.6	80.4	318	0	9038.4	314.6	338.3	23.7
9042.6	80.1	318	0	9038.5	311.5	338.3	26.8
9042.6	80.1	318	0	9039.4	312.6	338.3	25.7
9042.6	80.1	318	0	9039.6	311.3	338.4	27.1
9042.6	80.3	318	16.2	9037.9	315.7	338.3	22.6
9042.6	80.2	318	0	9037.7	312	338.3	26.3
9042.6	80.2	318	0	9037.7	310.9	338.3	27.4
9042.6	80.1	318	0	9038.2	312.9	338.3	25.4
9042.6	80.1	318	0	9042.1	311.2	338.4	27.2
9042.6	80	318	0	9042.2	309.8	338.4	28.6
9042.6	80	318	0	9042.4	306.7	338.4	31.7
9073.1	4.9	318	0	9070.1	321.8	339.1	17.3
9073.1	80.6	318	0	9070.5	321.4	339.1	17.7
9073.1	80.5	318	0	9071.5	312.5	339.1	26.6
9117.9	80.7	318	12.4	9114.7	329.7	340.2	10.5
9117.9	80.6	318	10.8	9114.8	311.8	340.2	28.4
9117.9	80.3	318	0.2	9114.9	313.5	340.2	26.7
9117.9	80.1	318	0	9115.2	313.1	340.2	27.1
9117.9	80.1	318	0	9115.6	313.4	340.2	26.8
9117.9	80.1	318	0	9115.8	313.8	340.2	26.4
9163.1	35.5	318	0	9159.3	328.6	341.3	12.7
9163.1	81	318	0	9159.6	322.6	341.3	18.7
9163.1	80.4	318	0	9160.9	317.7	341.3	23.6
9163.1	80.2	318	0	9161.1	318.3	341.3	23.0

Comparison of field measured value and calculated value

To compare the predicted values and field measured values both are graphically presented with respect to measured depth. HL in this case are considered for the depth between 8770 ft and 9180 while flow rate was consistent with 318 gpm. Figure 4.9 represents the comparisons between predicted values and measured values. According to Figure 4.5 all the way through the distance predicted values using the model shows steady trend with HL around 26.5 kips. Field measured value on the other hand comparing with the predicted value is lower for most of the interval.

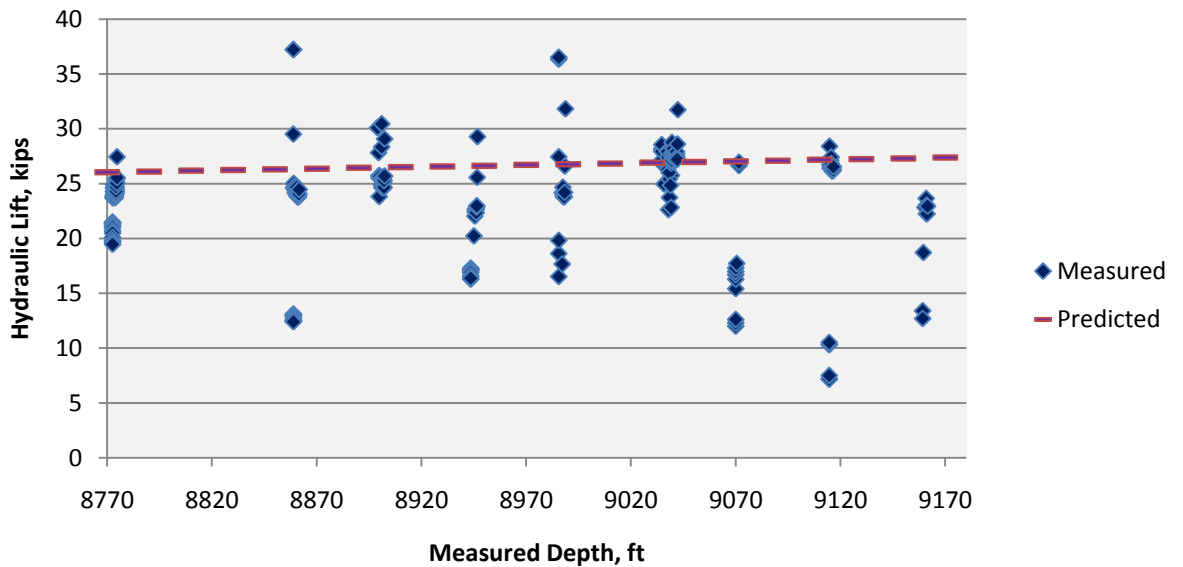


Figure 4.9: Comparison between measured HL and predicted HL for depth 8770ft – 9180 ft with flow rate 318 gpm

Analysis of the study

The calculated result for flow rate 318 gpm within depth 8770 ft to 9180 ft is compared with the real field data. Real field measured values are found considerably lower than the predicted values throughout the distance measured. HL model is derived as a function of frictional pressure drop and hydrostatic pressure differential while using the model calculation is performed considering uniform annulus with effective density including cuttings effect. This variation is due to some natural down hole fluid loss during mud circulation. In prediction calculation was performed with constant flow rate but this fluid loss causes minor reduction of fluid volume and reduced the frictional forces on casing wall. So it can be interpreted that there was no obstacles in the wellbore. In the field report and observation it also implies after using additives and cleaning the BHA drilling was quite consistent with sufficient hole cleaning from depth 8780 ft prior to reach 9204 ft. And there was no indication of significant loss circulation. Therefore, from this analysis derived HL model can be considered valid for this case as well.

4.3.3 Study of HL using the model at depth 9190-9204 ft- Section III

At this interval flow rate was maximized from 318 gpm to 342 gpm and continued drilling to reach 9204 ft. To analyze this case HL was also measured for this interval.

Prediction of HL using the model – Section III

Using the same model HL is measured for this last section. Table 4.14 shows the parameter used in equation (3.2) from Appendix A and B. Results obtained for this interval is tabulated in Table 4.15. Graphical representation of the HL shows the similar upward trend with depth Figure 4.10.

Table 4.14: Parameter used in the model for flow rate 342 gpm

Frictional pressure drop zone-A, $\left(\frac{dp}{dl}\right)_A$	0.042 psi/ft
Frictional pressure drop zone- B, $\left(\frac{dp}{dl}\right)_B$	0.079 psi/ft
Effective mud density, ρ_e ,	8.83 lbm/gal

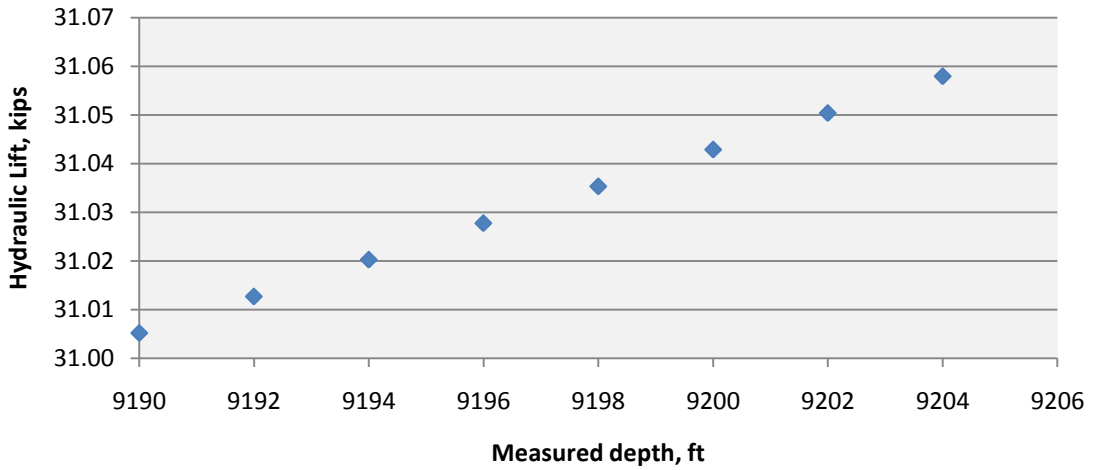


Figure 4.10: HL vs Measured depth at flow rate 342 gpm

Table 4.15: HL calculation for 9190 ft -9204 ft

Measured Depth.ft	Depth from 9-5/8 casing,ft	Clean Mud density, lbm/gal	Cuttings concentration	Effective mud density, lbm/gal	Plastic viscosity	Yield Point	Casing dia, inch	Hole dia, inch	Constant Flow rate, gpm	Annular Velocity, ft/s	Hedstrom number for Bingham Plastic model	Reynolds number	Friction factor	Anular frictional pressure drop, psi/ft	Total frictional pressure drop, psi/ft	Drag Force due to annular flow, lbf	Upward force at the bottom due to annular pressure drop, lbf	Force due to hydrostatic pressure differential in mud column, lbf	End force, lbf	Total HL lift, Kips
D	D _A	ρ_m	C _c	P _e	μ_v	YP	d _c	d _h	Q	V _a	He	N _{re}	ff	dp/dl		F ₁ , lb	F _{2_a} , Lbf	F _{2_b} , lbf	F ₂ = (F _{2_a} +F _{2_b})	(F ₁ + F ₂),
1700	0	8.8	0.0024	8.83	6	10	7	8.84	342	4.81	203306	9795	0.008	0.042	0.03	715				
9190	7490	8.8	0.0024	8.83	6	10	7	8.5	342	6.01	135850	10007	0.008	0.079	0.070	4895	24807	588	25395	30.76
9192	7492	8.8	0.0024	8.83	6	10	7	8.5	342	6.01	135850	10007	0.008	0.079	0.070	4897	24813	588	25401	30.77
9194	7494	8.8	0.0024	8.83	6	10	7	8.5	342	6.01	135850	10007	0.008	0.079	0.070	4898	24819	588	25407	30.78
9196	7496	8.8	0.0024	8.83	6	10	7	8.5	342	6.01	135850	10007	0.008	0.079	0.070	4899	24825	589	25414	30.78
9198	7498	8.8	0.0024	8.83	6	10	7	8.5	342	6.01	135850	10007	0.008	0.079	0.070	4901	24831	589	25420	30.79
9200	7500	8.8	0.0024	8.83	6	10	7	8.5	342	6.01	135850	10007	0.008	0.079	0.070	4902	24837	589	25426	30.80
9202	7502	8.8	0.0024	8.83	6	10	7	8.5	342	6.01	135850	10007	0.008	0.079	0.070	4903	24843	589	25432	30.81
9204	7504	8.8	0.0024	8.83	6	10	7	8.5	342	6.01	135850	10007	0.008	0.079	0.070	4904	24849	589	25438	30.81

Measurement of HL using field procedure – Section III

Results obtained for the interval 9190-9205 ft with flow rate 342 gpm are listed in Table 4.16.

Table 4.16: Field measurement of HL at depth 9190 ft- 9204ft and flow rate 342gpm

Timestamp	Hole Depth	Hook Load	Rotary RPM	Total Pump Output	Weight on Bit	Bit Depth	Hook Load	Hook load pump off	HL
2015-02-05T09:29:40	9204.1	315.2	80.1	343.5	0	9195.4	315.2	342.19	26.99
2015-02-05T09:58:50	9204.1	316	80	342.3	0	9195.4	316.0	342.19	26.19
2015-02-05T10:10:50	9204.1	316	80.1	342.3	0	9195.4	316.0	342.19	26.19
2015-02-05T10:11:20	9204.1	315.9	80.1	342.3	0	9195.4	315.9	342.19	26.29
2015-02-05T10:11:30	9204.1	316	80	342.3	0	9195.4	316.0	342.19	26.19
2015-02-05T10:25:30	9204.1	315.4	80	342.3	0	9195.4	315.4	342.19	26.79
2015-02-05T10:25:40	9204.1	315.5	80.1	342.3	0	9195.4	315.5	342.19	26.69
2015-02-05T10:35:40	9204.1	316.2	80.3	342.3	0	9196.7	316.2	342.22	26.02
2015-02-05T10:35:50	9204.1	316.2	80.2	342.3	0	9197.5	316.2	342.24	26.04
2015-02-05T10:36:00	9204.1	315.9	80.1	342.3	0	9198.4	315.9	342.26	26.36
2015-02-05T10:36:10	9204.1	317.3	80.1	342.3	0	9199.7	317.3	342.29	24.99
2015-02-05T10:36:20	9204.1	314.9	80.1	342.3	0	9199.7	314.9	342.29	27.39
2015-02-05T10:36:30	9204.1	314.3	80.0	342.3	0	9199.7	314.3	342.29	27.99
2015-02-05T10:37:00	9204.1	314	80.1	342.3	0	9199.7	314.0	342.29	28.29
2015-02-05T10:37:10	9204.1	314.1	80.1	342.3	0	9199.7	314.1	342.29	28.19
2015-02-05T12:04:00	9204.1	314.2	27.4	342.3	0	9190.6	314.2	342.07	27.87
2015-02-05T12:04:10	9204.1	314.2	27.3	342.3	0	9191.7	314.2	342.10	27.90
2015-02-05T12:04:20	9204.1	315.4	27.2	342.3	0	9193.4	315.4	342.14	26.74
2015-02-05T12:04:30	9204.1	311.1	27.0	342.3	0	9195.2	311.1	342.18	31.08
2015-02-05T12:04:50	9204.1	315.6	27.2	342.3	0.6	9198.9	315.6	342.27	26.67
2015-02-05T12:05:00	9204.1	319	27.2	342.3	0	9199.6	319.0	342.29	23.29
2015-02-05T12:05:10	9204.1	314.5	27.4	342.3	0	9200.8	314.5	342.32	27.82
2015-02-05T12:05:20	9204.1	312.8	27.2	342.3	0	9202.5	312.8	342.36	29.56
2015-02-05T12:05:30	9204.1	318	26.9	342.3	0	9202.5	318.0	342.36	24.36
2015-02-05T12:05:40	9204.1	320.7	3.0	86.2	0	9202.7	320.7	342.37	21.67

Comparison of field measured value and calculated value

To compare the predicted values and field measured values both are plotted with respect to depth. Figure 4.11 shows the results within the interval between 9190 ft to 9204 ft. All the way through the distance predicted values using the model shows steady trend with HL around 26.5 kips. Field measured value on the other hand comparing with the predicted value is lower for most of the interval.

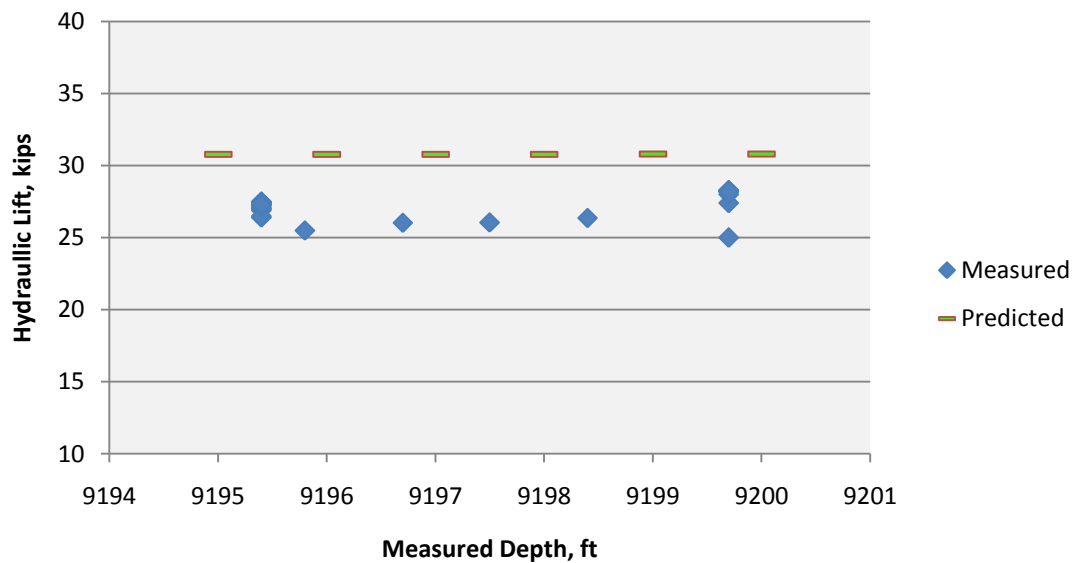


Figure 4.11: Comparison between measured HL and predicted HL for depth 9190 ft – 9204 ft with flow rate 342 gpm

Analysis of the study

This study is made for further analysis of the model with real field value. Similar feature is observed for this case as well after cleaning operation took place. Similarly, like case-II field values obtained for maximum flow rate 342 gpm are also lower compare to the predicted value for the distance measured. This attribute is also can be interpret from the field reports. So, from the analysis it can be said that derived hydraulic model shows convincing output for different cases and It can be used to monitor the well bore condition during CwD operation.

Chapter 5: Conclusion

In this study focus has been given to derive the theoretical model of overall hydraulic lift force during CwD operation. This is mainly to monitor the wellbore condition during casing drilling. In this work hydraulic lift is modeled as a function of annular frictional pressure drop. Hydrostatic pressure differential of annular mud column also has influential effect on total force. Deviation of the field's measured hydraulic lift values from the predicted values is an indicator of the wellbore distortions.

Upon studying different cases of a vertical well it can be summarized that according to the hydraulic lift principles fluid velocity rises with the reduction of flowing area which leads to higher frictional pressure drop. So higher hydraulic lift measured using field method implies that fluid flow hindered due to any obstacle in wellbore. Thus, higher lifting force compared to the predicted value using theoretical model for a certain interval depth is an indicator of wellbore irregularities and poor hole cleaning as well. This phenomenon has been verified with the real field case.

In this whole analysis the effect of tool joints, eccentricity of the casing in the well has been ignored to simplify the model. But in CwD these factors may eventually play important role in frictional pressure drop calculation which is a function of hydraulic lift. So, this factor can be used in future to improve the model. Hydraulic lift model only for the vertical well is analyzed in this study. Due to lack of data it has not been possible to validate for the inclined well. So it is recommended to verify the model for inclined well with the real data.

Reference:

- Bourgoyne Jr, A.T., Millheim, K.K., Chenevert, M.E. and Young Jr, F.S. (1986) "Applied Drilling Engineering". Vol. 2
- Galloway, G. (2004) "Cement in place drilling with casing system provides safe, reliable method for improving drilling efficiency," Paper OTC 16565 presented at Offshore Technology Conference, Houston, Texas, May 3-6
- Gupta, A.K. (2006). "Drilling with casing: Prospects and limitations," Paper SPE 99536 presented at the SPE Western Regional/AAPG Pacific Section/GSA Cordilleran Section Joint Meeting, Anchorage, Alaska, May 8-10
- Karimi, M., Petrie, S., Moellendick, E., and Holt, C. (2011). "A review of casing drilling advantages to reduce lost circulation, improve wellbore stability, augment wellbore strengthening, and mitigate drilling-induced formation damage," Paper SPE/IADC 148564 presented at the SPE/IADC Middle East Drilling Technology Conference and Exhibition, Muscat, Oman, 24-26 October
- Karimi, M., Moellendick, E., and Pena, C. (2012). "Casing drilling allows for safer engineering design," Paper AADE-12-FTCE-19 was presented at the AADE Drilling Fluids Technical Conference, Houston, Texas, 10-11 April.
- Kenga, Y., Atebe, J., and Feasey, G. (2009). "Successful implementation of 9 5/8-in. casing drilling in Nigeria: Case history of AKAMBA-2," Paper SPE 128890 presented at Nigeria Annual International Conference and Exhibition, Abuja Nigeria, 3-5 August
- Lopez, E.A., Bonilla, P.A., (2010) "Casing Drilling Application in the Depleted La Cira Infantas Mature Field Colombia", SPE 139020, SPE Latin American & Caribbean Petroleum Engineering Conference, Peru, December 1-3.

- Rosenberg, S., Gala, D.M., and Xu, W. (2010). "Liner drilling technology as mitigation to hole instability and loss intervals: A case study in the gulf of Mexico," Paper SPE/IADC 128311 presented at the SPE/IADC Drilling Conference and Exhibition, New Orleans, Louisiana, 2-4 February.
- Sanchez, F., and Al-Harthy, M.H. (2011). "Risk analysis: Casing-while-Drilling (CwD) and modeling approach," Journal of Petroleum Science and Engineering, Vol. 78.
- Tessari, R.M., Warren, T.M., and Jo, J.Y. (2006). "Drilling with casing reduces cost and risk," Paper SPE 101819 presented at the SPE Russian Oil and Gas Technical Conference and Exhibition, Moscow, Russia, October 3-6
- Warren, T., and Lesso, B. (2005). "Casing drilling directional wells," Paper OTC 17453 presented at Offshore Technology Conference, Houston, Texas, May 2-5

Appendices

Appendix- A

Calculation for Vertical Well Zone- A Section 1

$$\begin{aligned}\text{Annular Velocity,} &= \frac{q}{2.448(d_2^2 - d_1^2)} \\ &= \frac{293}{2.448(8.835^2 - 7^2)} \\ &= 4.12 \text{ ft/sec}\end{aligned}$$

Hedstrom Number, N_{He} :

$$\begin{aligned}&= \frac{24700\rho v(d_{hA} - d_c)^2}{\mu_p^2} \\ &= \frac{24700 \times 8.8 \times 4.12(8.835 - 7)^2}{6^2} \\ &= 203306\end{aligned}$$

Critical Reynolds number, N_{Re}

$$\begin{aligned}&= \frac{752\rho v(d_{hA} - d_c)}{\mu_p} \\ &= \frac{757 \times 8.8 \times (8.835 - 7)}{6} \\ &= 8392\end{aligned}$$

Now from the figure for flow criteria of bingham plastic fluid,

Critical Reynolds number, $N_{Re} >$ Hedstorm number, So the flow pattern is turbulent.

Friction factor for turbulent flow, f_f :

$$\begin{aligned}&= \frac{0.791}{N_{Re}^{0.25}} \\ &= \frac{0.791}{8392^{0.25}} \\ &= 0.008\end{aligned}$$

$$\begin{aligned}
 \text{Annular frictional pressure drop, } \left(\frac{dp}{dl} \right)_A &= \frac{\rho f_f v^2}{21.2(d_{hA} - d_c)^2} \\
 &= \frac{8.8 \times 0.008 \times 4.12^2}{21.2(8.835 - 7)^2} \\
 &= 0.032 \text{ psi / ft}
 \end{aligned}$$

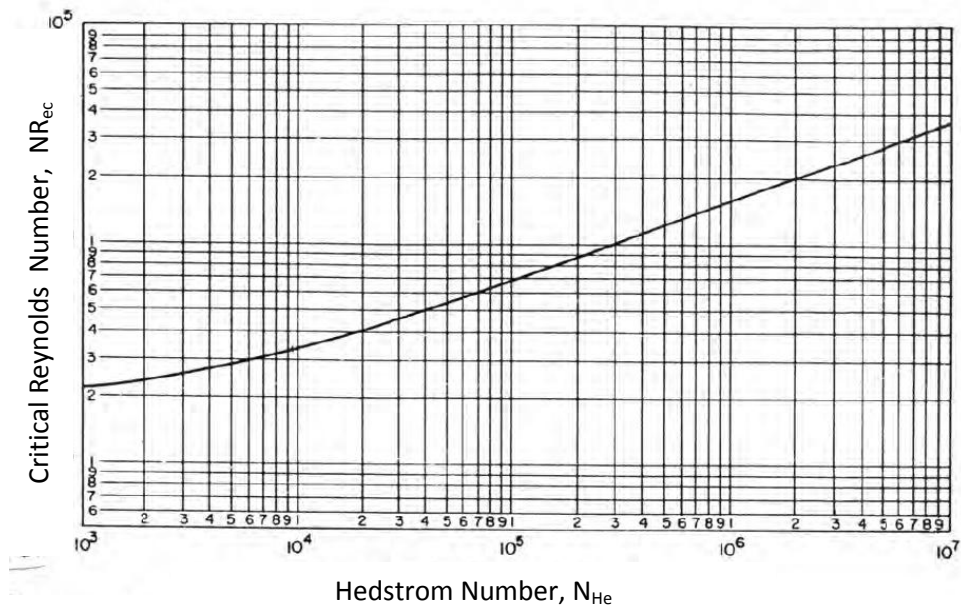


Figure A: Critical Reynolds number for Bingham plastic fluids

Similarly, annular frictional pressure drop for zone B,

$$\left(\frac{dp}{dl} \right)_B = 0.06 \text{ psi / ft}$$

Appendix- B

Effective mud density calculation

To determine the effective mud density it is necessary to calculate cuttings concentration. Here cutting concentration is calculated using average ROP 20.8 ft/hr and assuming particle size 0.25 inch. During drilling formation water and will added to the mud. Therefore considering porosity 0.15 and water saturation 0.2 cuttings concentration is determined.

Density of mixed fluid

Formation being drilled at a rate

$$\begin{aligned} \text{ROP} &= 20.8 \times \frac{\pi \times 7^2}{4 \times 144} \times \frac{7.48}{60} \\ &= 0.69 \text{ gal / min} \end{aligned}$$

Formation water is being added to the drilling fluid at a rate,

$$\begin{aligned} &= 0.69 \times 0.15 \times 0.20 \\ &= 0.027 \text{ gal/min} \end{aligned}$$

Solid being added to the at a rate,

$$\begin{aligned} &= 0.63 \times (1-0.15) \\ &= 0.59 \text{ gal/min} \end{aligned}$$

Hence, density of the mixture,

$$\begin{aligned} \rho_f &= \frac{\sum \rho_i V_i}{\sum V_i} \\ &= \frac{(8.8 \times 293) + (21.6 \times 0.59) + (0.027 \times 8.33)}{293 + 0.59 + 0.027} \\ &= 8.08 \text{ lbm / gal} \end{aligned}$$

Cuttings concentration determination

At first particles slip velocity (V_{sl}) is calculate. Here Chein's correlation is used to calculate V_{sl} ,

Condition 1

Assuming transitional flow pattern,

For Reynolds number $N_{Re} < 100$

$$N_{Re} = \frac{928 \rho_f V_{sl} d_s}{\mu_p}$$

Now particles slip velocity,

$$V_{sl} = 0.0075 \times Z \times \left[\sqrt{1 + \left(36800 \frac{d_s}{Z^2}\right) + \frac{(\rho_s - \rho_f)}{\rho_f}} - 1 \right]$$

$$\begin{aligned} \text{Here, } Z &= \frac{\mu_p}{\rho_f d_s} \\ &= \frac{6}{8.08 \times 0.25} \\ &= 2.97 \end{aligned}$$

Hence, the slip velocity,

$$\begin{aligned} V_{sl} &= 0.0075 \times 2.97 \times \left[\sqrt{1 + \left(36800 \frac{0.25}{2.97^2}\right) + \left(\frac{21.6 - 8.08}{8.08}\right)} - 1 \right] \\ &= 0.9860 \end{aligned}$$

So, Reynolds Number,

$$\begin{aligned} N_{Re} &= \frac{928 \times 8.08 \times 0.698 \times 0.25}{6} \\ &= 218 \end{aligned}$$

Here, $N_{Re} > 100$ so this assumption ($N_{Re} > 100$) is not appropriate.

Condition 2

For N_{Re} above 100 Chein recommends to use friction factor $f_f=1.72$ for slip velocity V_{sl}

$$\begin{aligned} \text{Particles slip velocity, } V_{sl} &= 1.89 \sqrt{\left\{ d_s \times \frac{(\rho_s - \rho_f)}{\rho_f f_f} \right\}} \\ &= 0.93 \end{aligned}$$

$$\begin{aligned} \text{Reynolds Number, } N_{Re} &= \frac{928 \times 8.08 \times 0.93 \times 0.25}{6} \\ &= 291 \end{aligned}$$

Reynolds number in this case is above 100.

Thus the particle slip velocity is 0.93 ft/sec

Now, cuttings transport ratio,

$$\begin{aligned} F_T &= \left(1 - \frac{V_{sl}}{v}\right) \\ &= \left(1 - \frac{0.93}{5.15}\right) \\ &= 0.82 \end{aligned}$$

Cuttings Concentration

$$\begin{aligned} C_c &= \frac{ROP \times d_c^2}{1466.95 \times F_T \times q} \\ &= \frac{20.8 \times 7^2}{1466.95 \times 0.82 \times 293} \\ &= 0.0029 \end{aligned}$$

Effective density,

$$\begin{aligned} \rho_e &= \rho_m(1 - C_c) + \rho_s C_c \\ &= 8.8 \times (1 - 0.29) + (21.6 \times 0.29) \\ &= 8.84 \end{aligned}$$

Now, using equation 3.2 HL can be obtained. Here, at depth 8713 ft,

$$\begin{aligned}
HL &= \left\{ \left(\frac{d_{hA} - d_c}{4} \right) \times \left(\frac{d_p}{d_l} \right)_A \times 2\pi \times \frac{d_c}{2} \times D_A \right\} + \left\{ \left(\frac{d_{hB} - d_c}{4} \right) \times \left(\frac{d_p}{d_l} \right)_B \times 2\pi \times \frac{d_c}{2} \times (D - D_A) \right\} \\
&+ \\
&\left[\left\{ \left(\frac{d_p}{d_l} \right)_A \times D_A \right\} + \left\{ \left(\frac{d_p}{d_l} \right)_B \times (D - D_A) \right\} + \left\{ 0.052 \times d_c^2 (\rho_e - \rho_m) \times D \right\} \right] \times \frac{\pi}{4} \times d_c^2 \\
&= \left\{ \left(\frac{8.835 - 7}{4} \right) \times 0.032 \times 2 \times 3.14 \times \frac{7}{2} \times 1700 \right\} + \left\{ \frac{8.5 - 7}{4} \times 0.06 \times 3.14 \times 7 \times (8713 - 1700) \right\} \\
&+ \\
&\left[\{0.032 \times 1700\} + \{0.06 \times (8713 - 1700)\} + \{0.052 \times 7^2 \times (8.84 - 8.8) \times 8713\} \right] \times 0.785 \times 7^2 \\
&= 22980 \text{ lbf} \\
&= 22.98 \text{ kips}
\end{aligned}$$

Using similar procedure HL for any depth can be calculated for this well. Parameters determined for each case are tabulates in Table-A

Table A – Set of parameters determined for HL lift prediction

Parameter	Section-I	Section-II	Section-III
Flow Rate, q	293	318	342
Pressure drop $\left(\frac{dp}{dl} \right)_A$	0.032	0.035	0.042
Pressure drop $\left(\frac{dp}{dl} \right)_B$	0.06	0.00	0.073
Cuttings Concentration, Cc	0.0029	0.0026	0.0024
Effective mud density, ρ_e	8.84	8.83	8.83